Characterization of Ion Plating

A Major Project Report

Submitted in Partial Fulfillment for the Award of the Degree of

Master of Technology

In

Mechanical Engineering

With specialization in

PRODUCTION ENGINEERING

By

KALPANA GUPTA
(Roll No. 2K11/PIE/07)

Under the guidance of

Dr.A.K.Madan (Associate Professor)

&

Mr.Shailesh Mani Pandey (Assistant Professor)

Department of Mechanical Engineering

DEPARTMENT OF MECHANICAL AND PRODUCTION ENGINEERING

DELHI TECHNOLOGICAL UNIVERSITY

DELHI-110042

SESSION 2011-13

CERTIFICATE

This is to certify that the project entitled "**CHARACTERIZATION OF ION PLATING**" being submitted by me, is a bonafide record of my own work carried by me under the guidance and supervision of **Dr.A.K.Madan (Associate Professor)** & **Mr.Shailesh Mani Pandey** (Assistant Professor) in partial fulfillment of requirements for the award of the Degree of Master of Technology (Production Engineering) in Mechanical Engineering, from Delhi Technological University, Delhi.

The matter embodied in this project has not been submitted for the award of any other degree.

Kalpana Gupta

Enroll No: DTU/11/303

University Roll No: 2K11/PIE/07

This is to certify that the above statement made by the candidate is correct to the best of our knowledge.

Dr.A.K.Madan
(Associate Professor)
(SUPERVISOR)

Mr.Shailesh Mani Pandey
(Assistant Professor)
(CO-SUPERVISOR)

DEPARTMENT OF MECHANICAL AND PRODUCTION ENGINEERING
DELHI TECHNOLOGICAL UNIVERSITY
DELHI-110042

27-JUNE-13

2011-2013

ACKNOWLEDGEMENT

I have a great pleasure in expressing my deep sense of gratitude and indebtedness to **Dr. A.K.Madan (Associate Professor)** & **Mr.Shailesh Mani Pandey** (Assistant Professor) of Mechanical Engineering Department, Delhi Technological University, Delhi for their continuous guidance and invaluable suggestion and time at all stages from conceptualization to experimental and final completion of this project work. They have guided me for fundamentals and provided many technical papers on the subject matter and thus inculcated the interest and quest for knowledge of this work. He provided constant support and encouragement for successful completion of this work.

I am also grateful to **Prof. Naveen Kumar** Head Department of Mechanical Engineering, for providing the experimental facilities in various labs of the Department.

I also have great respect and indebtedness for **Mr. Rajesh Bora** and **Mr. Aman Kumar (Technician SEM & XRD),** for their support and facilities provided for experiments, required for the completion of this special subject.

My special thanks to **Dr. R.C.Singh** for his valuable time for guiding me and given his very useful critical comment on the work and help me to do the project work on time.

I am also thankful to all the lab assistants of my college for their kind help.

At the last but not the least to my friends **Mr. Sudeep Singh Baghel** and my family members who always give me strength and moral support to complete the work.

KALPANA GUPTA

CONTENTS

Title	**Page No.**
Certificate	
Acknowledgement	I
Abstract	II-III
Contents	IV-VIII
List of Figures	IX-XI
List of Tables	XII
Abbreviations	XIII
Chapter 1. Introduction	**1-33**
1.1. Internal Combustion Engine	1
1.2. Function of internal combustion engine	1-2
1.3. Component of internal combustion engine	2
1.3.1 Cylinder block	2
1.3.2 Cylinder Head	2
1.3.3 Piston	3
1.3.4 Piston Rings	3
1.3.5 Connecting Rod	4
1.3.6 Gudgeon Pin	4

1.3.7 Crank Pin 4

1.3.8 Crank Shaft 5

1.3.9 Cam Shaft 5

1.3.10 Inlet Valve & Exhaust Valve 5

1.3.11 Governor 5

1.3.12 Carburetor 5

1.3.13 Fuel Pump 5

1.3.14 Spark Plug 5

1.3.15 Fuel Injector 6

1.4 Types of Piston Rings 6-10

1.4.1 Compression rings 6

1.4.2 Oil control rings 6-10

1.5 Types of Piston Rings Material 10-11

1.6 Piston Rings Coatings 12-15

1.7 New Development in Piston Rings Coatings 16-17

1.8 Manufacturing 17-18

1.9 Testing on Piston Rings **18-23**

1.9.1 Chemical Composition 18

1.9.2 Coating Porosity 19

1.9.3 Pore Size 20

1.9.4 Microstructure and Phase distribution 20

1.9.5 Unmelted Particles and Reaction Products 21

1.9.6 Micro-cracks and Fissures 21

1.9.7 Coating Hardness 22

1.9.8 Particle and phase hardness 22

1.9.9 Running Face Porosity, Voids, Cracks, Bond Defects between Coating and Inlay Groove Land (on Inlaid Rings) 23

1.9.10 Coating Thickness 23-24

1.10. Types of wear of the coating 25-26

1.10.1 Adhesive wear of coating 24-33

1.10.2. Abrasive wears of coating 26-29

1.10.3. Surface fatigue wear of the coating 29-30

1.10.4. Fretting wear of coating 30-31

1.10.5. Erosive wear of coating 32-33

Chapter- 2 Testing on piston rings 34-49

2.1 Microstructure Testing 34

2.2 Chemical Composition Testing (using SEM/XRD/EDS) 34-35

2.3 Mechanical Strength (Micro Hardness) 35

2.4 Adhesion Testing 36

2.5 Wear testing on the piston rings Coatings 36-49

2.5.1 Types of wear test of piston rings coating 36-37

2.5.2 Scratch test of piston rings coating 37

2.5.3 Slurry Abrasion Test of piston rings coating 37-38

2.5.4 Friction Test of thermal spray coating 38-39

2.5.5 Air Jet Erosion Test of thermal spray coating 39-40

2.5.6 Pin on Disc Test of thermal spray coating 40-49

Chapter -3 Experimental Procedure **50-78**

3.1 Sample Preparation 50-53

3.2 Coating Preparation 54-60

3.2.1 Physical Vapor Deposition 54-56

3.2.2 Ion Plating 56-58

3.2.3 Stages of Ion Plating 59-60

3.3 Design of experiments 61-61

3.4 Pin on disc test 62-65

3.5 Scanning electron microscope 65-67

3.6 X -Ray diffractometer 67-68

3.7 Vickers micro hardness tester 69-70

3.8 Optical Microscope 70-71

Chapter -4 Result & Discussion **72-89**

4.1 Coating characterization 72-73

4.2. Wear rate of the Ion Plated Disc with Tungsten Carbide , HCS & Mild Steel 73-76

4.3. Coefficient of friction (CoF) of Ion Plated Disc with Tungsten Carbide, HCS & MS. 77-81

4.4 Wear mechanism of Ion Plated Disc with WC, HCS and Mild Steel 82-89

Chapter -5 Conclusion **90-91**

Chapter -6 Future Scope of this study **92**

Chapter -7 References **93-105**

LIST OF FIGURE

Sr. Number	Title	Page No.
Figure 1.1	Parts of Internal combustion engine	2
Figure 1.2	Position of different type of piston rings on piston	4
Figure 1.3	Most Common shape, b- barrel-shaped face profile, c- tapered face profile	8
Figure 1.4	Bevelled ring edge configuration (ISO 6621-1)	8
Figure 1.5	Half keystone ring (ISO 6621-1)	9
Figure 1.6	Compression & Oil Control Rings	9
Figure 1.7	Coating deposition technologies	13
Figure 1.8	Coating Porosity Calculations	19
Figure 1.9	Abrasive wear of Ion Plating coating	28
Figure 1.10	Fretting wear of Ion Plating coating	31
Figure 1.11	Erosion wear of Ion Plating coating	32
Figure 2.1	Slurry abrasions wear of Ion Plating coating	38
Figure 2.2	Pin on disc wear test of Ion Plating coating	40

Figure 3.1	Induction Arc Furnace Used for the Melting of Charge	51
Figure 3.2	Powder as charged (A) Mn Slab (B) Cu Powder (C) Si Powder (D) Cr Powder	52
Figure 3.3	PVD Processing Technique	55
Figure 3.4	Ion Plating Configurations	59
Figure 3.5	Wear and friction monitor machine for pin on disc test	62
Figure 3.6	Ion Plated Disc before wear test	63
Figure 3.7	Ion Plated Disc during wear test	63
Figure 3.8	Ion Plated specimen after wear test	64
Figure 3.9	Scanning electron microscope at DTU, Delhi	66
Figure 3.10	X-Ray diffractometer in DTU, Delhi	68
Figure 3.11	Vickers micro hardness indentations	70
Figure 3.12	Optical microscope	71
Figure 4.1	Top View of Ion Plating	72
Figure 4.2	(A) Shows the variation of the wear rate of the Ion Plated Disc at different loads with different counter bodies.	73
	(B) Shows the variation of the wear rate of the different counter bodies at different loads with Ion Plated Disc.	74
Figure 4.3	(A) Variation of coefficient of friction of Ion Plated Disc with WC pin at various loading and sliding conditions.	77
	(B) Variation of coefficient of friction of Ion Plated Disc with HCS pin at various loading and sliding conditions	77
	(C) Variation of coefficient of friction of Ion Plated Disc	78

with MS pin at various loading and sliding conditions

(D) Variation of coefficient of friction of Ion Plated Disc with WC, HCS and MS pin at 40 N loading and 550 rpm sliding conditions. 78

(E) Variation of coefficient of friction of Ion Plated Disc with WC, HCS and MS pin at 50 N loading and 650 rpm sliding conditions 79

(F) Variation of coefficient of friction of Ion Plated Disc with WC, HCS and MS pin at 70 N loading and 850 rpm sliding conditions 79

Figure 4.4 Worn surfaces Ion Plated Disc with WC at 550 rpm speed & 40N Load 81

Figure 4.5 EDS Graph of Wear Track of Ion Plated Disc with counter Body of WC 82

Figure 4.6 Worn surfaces of Ion Plated Disc with HCS pin at 750 rpm speed & 60 N Load 84

Figure 4.7 Worn surfaces of HCS pin against the Ion Plated Disc

Figure 4.8 Worn surfaces of HCS pin against the Ion Plated Disc 85

Figure 4.9 Worn surfaces of Ion Plated Disc with tungsten carbide at 550 rpm speed and 40N load 86 87

Figure 4.10 EDS Graph of Wear Track of Ion Plated Disc with counter Body of MS 88

ABBREVIATIONS

Symbol	Explanation
μ	co-efficient of friction
Φ	pin diameter
g	grams
Kg	kilogram
N	load in Newton
Hv	Vickers microhardness
μm	Micrometer
A°	Armstrong
d	Intermolecular distance
θ	Angle of incidence
3D	Three dimensional
D_1, D_2	Diagonals of indenter
Rpm	Revolution per minute
SEM	Scanning electron microscope
XRD	X-ray diffractometry
EDS	Electronic dispersive spectrometry

ABSTRACT

The functions of a piston ring are to seal off the combustion pressure, to distribute and control the oil, to transfer heat and to stabilize the piston. Most piston rings and metallic sealing rings for modern application require some form of coating, where running conditions are severe to minimise abrasion and corrosion. The piston ring coating improves the life of engine as well as fuel efficiency. In this study, Physical Vapour Deposition (Ion Plating) was investigated; Plates with similar composition as the piston ring material were prepared by the casting process using induction arc furnace and sand mould. The PVD having 99.9% Cr was used. PVD are now days preferred in the automobile industries. The cast iron substrate of same composition as of piston rings was used to get the similar result as in the engine cylinder piston combination. After preparation of the coating, the plate (90x90x2 mm) was prepared with the help of a surface grinder and a fixture was designed to hold the plate on the pin on disc machine. There are different wear tests such as scratch test, slurry abrasion test, erosion test and pin on the disc test. The selection of the wear test depends on the material of the coating and its applications. For marine applications of the coating, slurry erosion and corrosion test are preferred. But in case of dry applications of the coating the pin on disc and scratch test are commonly performed. In the present study two variables were selected for wear test: load (40 , 50, 60 & 70 N) , Sliding Speed (550, 650, 750 & 850 rpm) keeping the sliding distance 2000 m . Wear test of the coating was conducted on pin on disc machine under dry conditions. The wear rate was calculated using mass loss methods on an electronic balance having least count of 0.0001g. The coefficient of friction was found with LVDT which elucidated the frictional force during wear test. The

morphology of worn surfaces of the coating was analysed with scanning electron microscope. The XRD was done to determine the change in intermolecular spacing of the worn surfaces of the coating. The wear rate of the coating was found to be increased with increase in load as well as sliding speed for the Ion Plating with the counter body of tungsten carbide but in the case of Ion Plating with the HCS & MS it is found to be decreased.. However, the co-efficient of friction of the coating was found to decrease with increased load and sliding speed for all processes. The d-spacing of the coating molecules on the wear track was found to decrease with increased load. The microstructure of the worn surfaces of the coating was also examined with optical telescope and no change in microstructure of the coating due to frictional heat was found. The micro hardness at the cross section of the coating at wear track was found to decrease when moving away from the wear track. The main wear mechanisms observed by scanning electron microscope were adhesion, deformation and microcutting. The wear rate depends on the load applied. With the increase of applied load the wear rate found to be increased in the Ion plated with the counter body of Tungsten Carbide but with the counter body of HCS & MS it is found to be decreased. The Coefficient of friction was found to be decreased with the increase of load and sliding speed.

Key words: Air Plasma spray, pin on disc, microstructure, wear rate, Hard chrome plating.

CHAPTER ONE-INTRODUCTION

1.1 Internal Combustion Engines

The **internal combustion engine** is an engine in which the combustion of a fuel (normally a fossil fuel) occurs with an oxidizer (usually air) in a combustion chamber. In an internal combustion engine, the expansion of the high-temperature and high -pressure gases produced by combustion apply direct force to some component of the engine. This force is applied typically to pistons, turbine blades, or a nozzle. This force moves the component over a distance, transforming chemical energy into useful mechanical energy. The first internal combustion engine was created by Étienne Lenoir

The term internal combustion engine usually refers to an engine in which combustion is intermittent, such as the more familiar four-stroke and two-stroke piston engines, along with variants, such as the six-stroke piston engine and the Wankel rotary engine. A second class of internal combustion engines use continuous combustion: gas turbines, jet engines and most rocket engines, each of which are internal combustion engines on the same principle as previously described

1.2 Function of Internal Combustion Engine

Functions of I.C. Engine: Engine is that kind of prime mover which converts chemical energy of fuel into mechanical energy. The fuel on burning changes to gas which impinges upon the piston and pushes it to change into reciprocating motion. The reciprocating motion of piston is then converted to rotary motion of crank shaft with the help of slider mechanism involving connecting rod and crank shaft. Several types of

I.C. Engines are used on various automobiles i.e. marine, locomotive, air craft and other industrial applications.

1.3 Component of Internal Combustion Engine

1.3.1 Cylinder Block

Function- In the bore of cylinder the fresh charge of air-fuel mixture is ignited, compressed by piston and expanded to give power to piston.

1.3.2 Cylinder Head

Function-It carries inlet and valve. Fresh charge is admitted through inlet valve and burnt gases are exhausted from exhaust valve. In case of petrol engine, a spark plug and in case of diesel engine, an injector is also mounted on cylinder head.

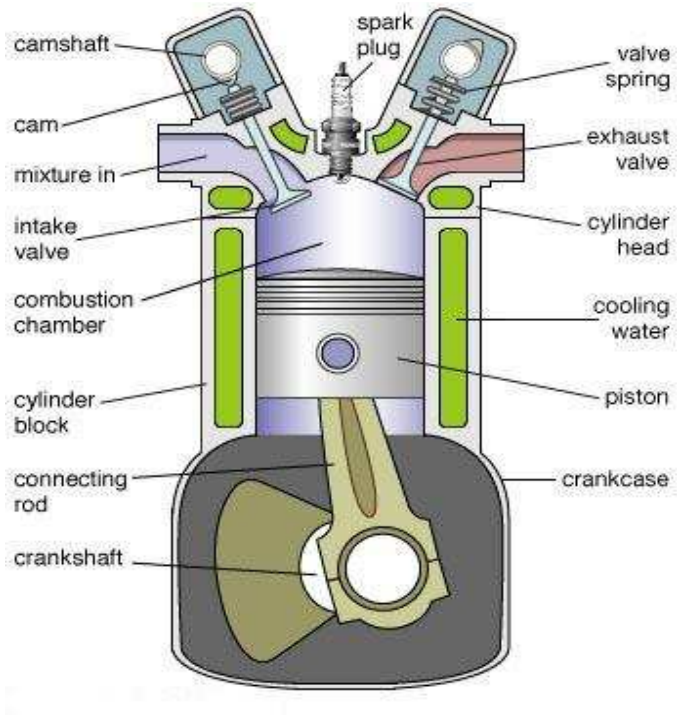

Figure 1.1 Parts of Internal combustion engine [97]

1.3.3 Piston

Function-During suction stroke, it sucks the fresh charge of air-fuel mixture through inlet valve and compresses during the compression stroke inside the cylinder. This way piston receives power from the expanding gases after ignition in cylinder. Also forces the burnt exhaust gases out of the cylinder through exhaust valve.

1.3.4 Piston Rings [60]

Piston Ring Functions and Operation

The functions of a piston ring are to seal off the combustion pressure, to distribute and control the oil, to transfer heat, and to stabilize the piston. The piston is designed for thermal expansion, with a desired gap between the piston surface and liner wall. The rings and the ring grooves form a labyrinth seal, which relatively well isolates the combustion chamber from the crankcase. The position and design of the ring pack is shown in Fig 1.2 The ring face conforms to the liner wall and moves in the groove, sealing off the route down to the crankcase. The sealing ability of the ring depends on a number of factors, like ring and liner conformability, pre-tension of the ring, and gas force distribution on the ring faces. Some of the combustion chamber heat energy is transferred through the piston to the piston boundaries, i.e. the piston skirt and rings, from which heat transfers to the liner wall. Furthermore, the piston rings prevent excess lubrication oil from moving into the combustion chamber by scraping the oil from the liner wall during the down stroke. The piston rings support the piston and thus reduce the slapping motion of the piston, especially during cold starts where the clearance is greater than in running conditions. The rings are generally open at one location, at the ring gap, hence easily assembled onto the piston; see Fig1. 2.

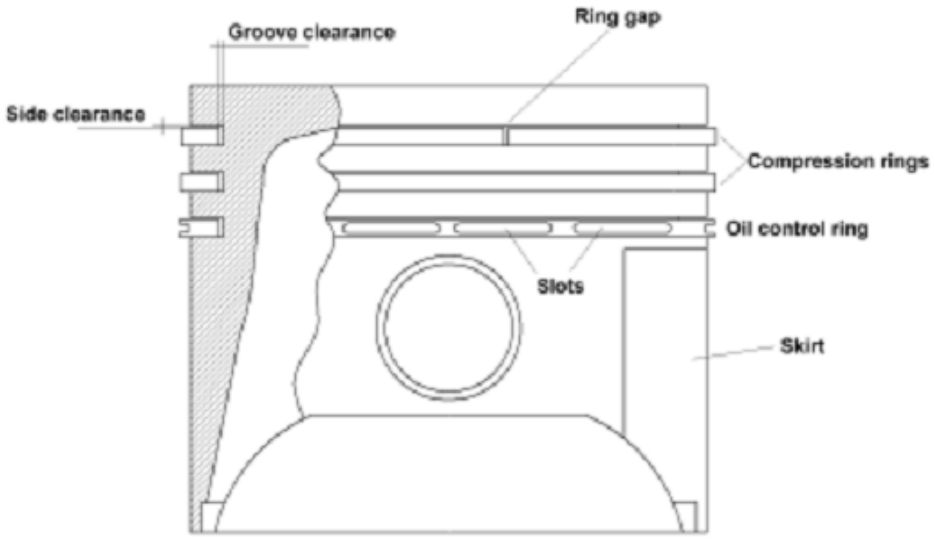

Fig 1.2 Position of different type of piston rings on piston [60]

Function-It prevents the compressed charge of fuel-air mixture from leaking to the other side of the piston. Oil rings, is used for removing lubricating oil from the cylinder after lubrication. This ring prevents the excess oil to mix with charge.

1.3.5 Connecting Rod

Function-It changes the reciprocating motion of piston into rotary motion at crankshaft. This way connecting rod transmits the power produced at piston to crankshaft.

1.3.6 Gudgeon Pin

Function- Connects the piston with small end of connecting rod.

1.3.7 Crank Pin

Function- Hand over the power and motion to the crank shaft which come from piston through connecting rod.

1.3.8 Crank Shaft

Function-Receives oscillating motion from connecting rod and gives a rotary motion to the main shaft. It also drives the camshaft which actuates the valves of the engine.

1.3.9 Cam Shaft

Function-It takes driving force from crankshaft through gear train or chain and operates the inlet valve as well as exhaust valve with the help of cam followers, push rod and rocker arms.

1.3.10 Inlet Valve & Exhaust Valve

Function-Inlet valve allow the fresh charge of air-fuel mixture to enter the cylinder bore. Exhaust valve permits the burnt gases to escape from the cylinder bore at proper timing.

1.3.11 Governor

Function-It controls the speed of engine at a different load by regulating fuel supply in diesel engine. In petrol engine, supplying the mixture of air-petrol and controlling the speed at various load condition.

1.3.12 Carburetor

Function-It converts petrol in fine spray and mixes with air in proper ratio as per requirement of the engine.

1.3.13 Fuel Pump

Function-This device supply the petrol to the carburetor sucking from the fuel tank.

1.3.14 Spark Plug

Function-This device is used in petrol engine only and ignites the charge of fuel for combustion.

1.3.15 **Fuel Injector**

Function-This device is used in diesel engine only and delivers fuel in fine spray under pressure.

1.4 Types of Piston Rings [60]

Piston rings form a ring pack, which usually consists of 2–5 rings, including at least one compression ring. The number of rings in the ring pack depends on the engine type, but usually comprises 2–4 compression rings and 0–3 oil control rings. For example, fast speed four-stroke diesel engines have 2 or 3 compression rings and a single oil control ring. The oil control rings used in diesel engines are two-piece assemblies and spark-ignited engine oil control rings may be three-piece assemblies as well. In addition to the general compression rings and oil control rings there are scraper rings, which have the tasks of both sealing and scraping off the oil from the liner wall. Scraper rings have a beak intended for scraping off the oil; see the Figs. 1.6a and 1.6b

1.4.1 Compression rings

The compression ring acts as a gas seal between the piston and the liner wall, preventing the combustion gases from trailing down to the crankcase. The rings have a certain pre-tension, i.e. they have a larger free diameter than the cylinder liner, which assists the ring in conforming to the liner. The cylinder gas pressure acts on the back-side of the ring, especially on the top ring, pressing it against the liner. The ring force distribution depends on the face form. With a rectangular face profile the force is higher than with a barrel-shaped face, as the compression pressure is able to act on the face-side of the barrel-shaped ring and thus counteract some of the force owing to ring pre-tension. Plain compression rings, with a rectangular cross-section, satisfactorily meet

the sealing demands of ordinary running conditions and this type of compression ring is the most common one, see Fig. 1.3a. The use of rings with a barrel-shaped face profile (Fig. 1.3b) brings the benefit mentioned above. The ring may have a tapered face profile in order to shorten the running-in period, see Fig. 1.3c. The tapered face profile enables the compression gas pressure to act on the face-side as well and thus relieve the pressure against the liner wall, which reduces the wear rate during running-in. A tapered face profile has a good oil-scraping ability, and the ring can be used as an oil-scraping ring as well as a compression ring Beveled rings can be used as compression rings, see Fig. 1.4. The bevelled profile causes the ring to twist in the ring groove during engine operation. In running conditions the bevelled ring is pressed flat against the liner wall owing to the gas pressure, which causes an additional stress on the ring. The wedge-type profile or (half) keystone profile is used in order to prevent the ring from seizing in the groove, see Fig. 1.5. High temperature may cause the lubricant in the groove to carbonize. The wedge form makes the ring´s axial clearance greater at increasing radial groove clearance. Scraper rings, which are usually used as the second compression rings, can simultaneously be used as oil-scraper rings, see the Figs. 1.6a and 1.6b.

1.4.2 Oil control rings

In addition to the task of the compression rings to seal off the combustion chamber from the crankcase, there needs to be some mechanism to distribute the oil evenly onto the liner. The number of oil control rings in a ring pack is one or two. Normally a single oil control ring is sufficient but on occasions a second ring may be required. The

appearance of the oil control ring differs from that of the compression ring; see the Figs. 1.6c and 1.6d.

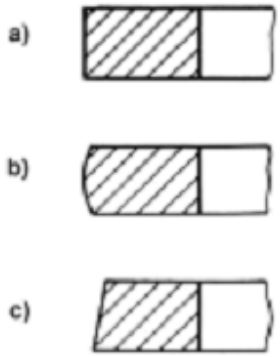

Figure 1.3 a- Most Common shape, b- barrel-shaped face profile, c- tapered face profile

Compression Ring cross-section (ISO 6621-1)

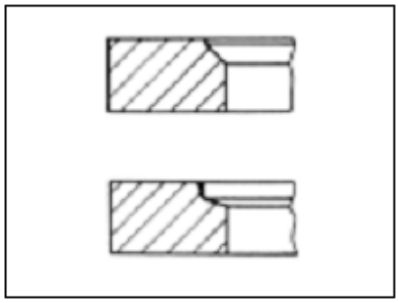

Figure 1.4

Bevelled ring edge configuration (ISO 6621-1)

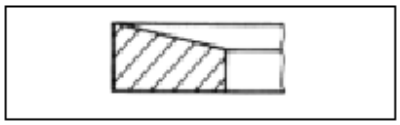

Figure 1.5

Half keystone ring (ISO 6621-1)

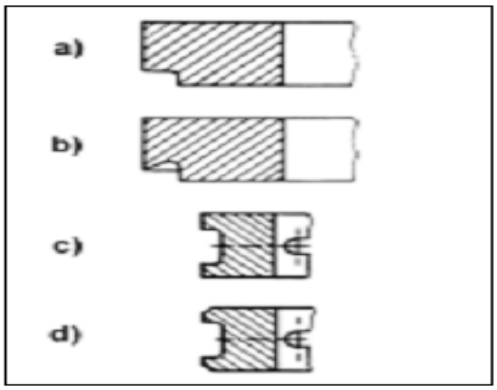

Figure 1.6 a, b, c, d

Compression & Oil Control Rings

The oil control ring is perforated by slots in the peripheral direction; see Fig. 2.1, which provides a way for the excess oil to leave the ring pack area. The scraped oil is collected in the oil control ring groove and transported through the piston back to the crankcase. The scraped oil may run through the possible gap between the liner wall and the piston skirt. With the latter alternative, the oil is forced in front of the oil control ring. The oil control rings may have a coil spring inserted, as the pre-tension of the ring is not

sufficient in all instances. The additional force on the oil control rings causes them to have the most extreme lubrication conditions, even though these are the rings that control the oil film. Oil control rings are not always necessary, contrary to the compression rings. Two-stroke spark-ignited engines, for example, have the lubrication oil mixed in the fuel, and therefore need no oil control rings.

1.5 Types of Piston Rings Material

A piston ring material is chosen to meet the demands set by the running conditions. Furthermore, the material should be resistant against damage even in emergency conditions. Elasticity and corrosion resistance of the ring material is required. The ring coating, if applied, needs to work well together with both the ring and the liner materials, as well as with the lubricant. As one task of the rings is to conduct heat to the liner wall, good thermal conductivity is required. Grey cast iron is used as the main material for piston rings [61].

From a tribological point of view, the grey cast iron is beneficial, as a dry lubrication effect of the graphite phase of the material can occur under conditions of oil starvation. Furthermore, the graphite phase can act as an oil reservoir that supplies oil at dry starts or similar conditions of oil starvation [62]

Alloyed grey cast irons is used in a heat-treated condition used for 2^{nd} groove. Besides having a high bending strength and modulus of elasticity, an increased hardness of 320 to 470 HB is produced in order to obtain the required wear resistance in the uncoated condition.

The demand for high wear strength is also met by the use of a tempered, alloyed cast iron . This has the benefit of a high bending strength of min. 800 MPa and high modulus of elasticity. The good wear resistance results from the combination of a fine-pearlitic matrix structure and finely dispersed, precipitated secondary carbides [63].

Unalloyed grey cast iron is used for 2-piece oil rings in the 3rd groove. These ring materials are characterized by a fine-lamellar graphite structure in a pearlitic matrix and have good conformability due to a relatively low modulus of elasticity.

Reduced width piston rings in gasoline engines to match reductions in the overall height of pistons, and increasing combustion pressures in diesel engines call for materials with increased strength characteristics.

These challenges are met by the use of high-chromium alloyed steels and spring steels. The greater durability under increased stresses is demonstrated by the improved fatigue strength manifested as form stability.

The wear resistance derives from finely distributed chromium carbides of the type $M_{23}C_6$ and M_7C_3 embedded in the tempered martensite matrix. For improved wear resistance these steelsare mainly used in a nitrided condition or with a peripheral coating.

The steels mentioned are used chiefly as compression ring materials for gasoline engines and truck diesel engines as well as for the steel rails and expander-spacers of oil control rings and for 2-piece profiled steel oil rings.

1.6 Piston Rings Coatings

Most piston rings and metallic sealing rings for today's modern application will require one of the following types of coating:

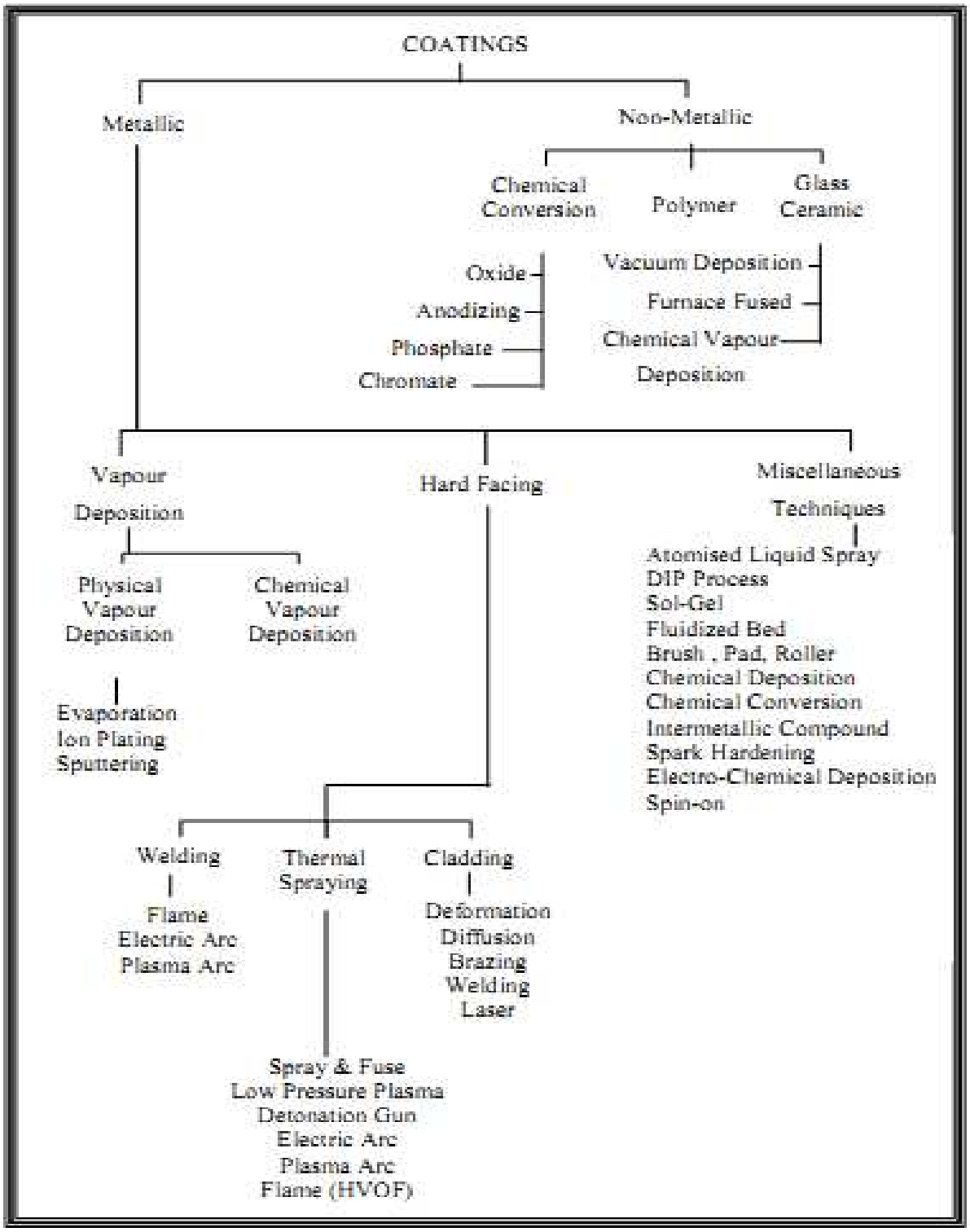

Figure 1.7 Coating deposition technologies [64]

Coatings for rings are widely used. One example of such a coating is chromium, which is used in abrasive and corrosive conditions where running conditions are severe. Hard chrome plating is particularly relevant for the compression ring.

Piston ring surfaces are, in addition to chromium plating, thermally (plasma) sprayed with molybdenum, metal composites, metal-ceramic composites or ceramic composites, as a uniform coating or an inlay coating material [65].

Experimental work with new powder compositions for thermal spraying has included molybdenum-nickel-chromium alloys, chromium oxide (Cr_2O_3) with metallic chromium binder, alumina-titania (Al_2O_3-TiO_2), tungsten carbide (WC) with metallic cobalt binder, $MoSi_2$, CrC-NiCr [66].

Hard chromium layers can be improved by plasma spraying chromium ceramic on the ring face, thus increasing the thermal load capacity. A dense chromium carbide coating, produced by HVOF coating was found promising for piston ring applications in the work by Rastegar and Richardson [67].

Thin, hard coatings produced by PVD or CVD include coating compositions like titanium nitride (TiN), chromium nitride (CrN); however coatings of this type are currently used exclusively for small series production for competition engines and selected production engines[68].

Multilayer Ti-TiN coatings have been experimentally deposited onto cast-iron piston rings, and the coating is claimed to be more wear resistant than a chromium plated or phosphate surface, particularly when the number of layers is high [69].

Haselkorn and Kelley have investigated coatings for use in low-heat rejection engines. They conclude that high carbon iron-molybdenum blend and chrome-silica composite applied by plasma spray, and further chrome nitride applied by low-temperature arc vapour are coatings with properties that meet the demands in low-heat rejection engines [70]

Surface coatings/treatments for the entire piston ring surface are based on phosphorus, nitrides, and ferro-oxides, copper and tin, as some examples [65].

The possibility of using ceramic piston rings as a complement to metallic rings in advanced engine applications has been investigated. Miniature tribo tests with ceramic materials have included monolithic zirconia, sintered silicon carbide, silicon nitride [71], and silicon nitride with a gradient of titanium nitride on the sliding surface [72]. Unlubricated sliding turned out to be detrimental to the ceramics. Silicon nitride and silicon carbide performed satisfactorily under oil-lubricated sliding conditions, while zirconia suffered from thermal shock cracking.

1.7 New Development in Piston Rings Coatings

Federal-Mogul Corporation has developed a new piston ring coating that supports vehicle manufacturers' efforts to make petrol engines more fuel-efficient.

The patented 'CarboGlide' coating delivers a claimed direct improvement in fuel economy and CO_2 emissions by reducing ring friction by up to 20% as compared to nitride or other commonly used coatings. Its high wear resistance will withstand an engine's full operational life - even in the latest generation of high-output petrol engines with turbocharging or direct injection. CarboGlide additionally protects the cylinder surface from scuffing and scoring, especially under the most critical lubrication conditions, because of its high chemical and physical stability, the supplier said.

The superior coating properties are achieved due to a multi-layer microstructure and a special coating composition that contains carbon, deposited in diamond-like form, as well as hydrogen and tungsten. The unique structure can be produced for a coating thickness of 10 microns, more than three times that of the industry's latest DLC coating. A specialised advanced process based on the combination of physical vapour deposition and plasma-assisted chemical vapour deposition, specifically developed for piston ring application, is used in applying CarboGlide. The coating's multi-layer architecture, together with the company's surface machining and finishing expertise, ensure the integrity of the coating structure, optimal adhesion of the coating and high coating stability on both steel and cast iron rings.

CarboGlide is Federal-Mogul's third and most advanced generation of the company's DLC coated ring technology. The coating was developed in Burscheid, Germany [73]

New Cr-based multilayer nitride hard coatings were developed by Teer Coatings Ltd., England, using a Teer UDP450/4 unbalanced DC magnetron sputter ion plating system. The coatings were incorporated with Ti, Al, V, Y, Mo and Cr metal target On the basis of the results of these tribological tests, the most promising coatings were determined according to an evaluation matrix and the further development was concentrated on these coatings [74].

1.8 Manufacturing

Grey cast iron and steel piston rings are manufactured in different processes. At some industry grey iron piston rings are cast as individual rings in a noncircular shape; there are other ring manufacturers who cut the individual rings from pots or cuffs. The rings are generally machined to the required shape by means of double cam turning, a process in which the ring blank, already axially ground, is copy turned simultaneously on the inside and outside diameters. After a segment equivalent to the free gap is cut from the ring it assumes the free shape that will give it the required radial pressure distribution when fitted into the cylinder. Once inside the cylinder the ring is completely light tight on its outside diameter and exerts the predefined radial pressure against the cylinder wall.

Besides using double cam turning, ring blanks can also be shaped by machining the inside and outside diameters separately. This involves cam turning the outside diameter

of the noncircular blank and machining the inside diameter with the ring in the compressed state. The gap is cut out in a step between O.D. and I.D. machining. Heat forming as a means of shaping piston rings should be mentioned to complete the range of options, but this process is seldom used.

Steel piston rings are made from a profiled wire. The rings are first coiled into a circular shape and then the gap is cut out. The necessary shape is obtained using a heat treatment process in which the rings are mounted onto an arbor appropriately designed to impart the required radial pressure distribution.

Profiling of the running faces of taper faced, Napier and slotted oil rings is carried out, depending on the ring design, on automatic O.D. lathes or profile grinding machines using special profile cutting tools before or after coating.

1.9 Testing on Piston Rings:

The various types of testing performed on the piston rings are mentioned below,

1.9.1 Chemical Composition

The spray coating is removed from the ring for analysis by stretching the ends of the ring apart or striking it until the coating comes free. The coating is then crushed. If the coating is contaminated with base material the analysis must be suitably corrected. The analysis is performed using analytical procedures (e.g. AAS) appropriate to the elements being tested.

1.9.2 Coating Porosity

The porosity of spray coatings is evaluated on the un-etched microsection. It is important for the evaluation to be carried out on representative areas of the coating. In the case of inlaid spray coatings the areas near to the inlay groove walls are not to be considered as representative because in these regions turbulence is generated in the spray jet during spraying and this can result in greater porosity. The specifications define maximum values for the porosity of representative areas of coating on full-face sprayed, half-inlaid and fully inlaid piston rings.

The porosity in the inlay groove wall region may be twice the value of the representative area. The size of the inlay groove wall region y is defined by the function y = cx, where c is an empirically determined constant and x the actual coating thickness. **For the inlay groove wall designs used up to now the value for c is 1.25.**

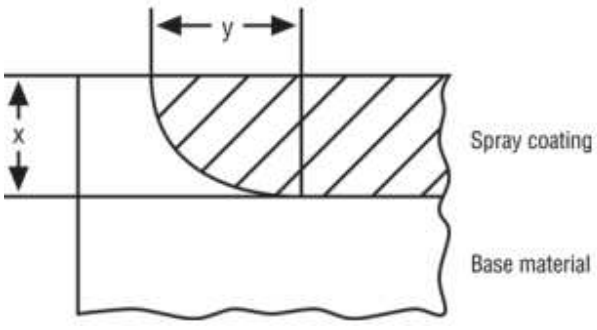

Figure 1.8, Coating Porosity Calculation

a) The pores in the coating areas are measured with a quantitative image analyzer. The surface area of all measured pores is set in relation to the area of the measurement field. The average of 30 measurement fields with a cumulative area of about 1.5 mm^2 is calculated for each ring.

b) The pores in the coating areas are estimated by comparing them against a classification chart containing photomicrographs of known porosities.

1.9.3 Pore Size

Pore sizes are stated as a size distribution percentage. All pores in representative measurement fields are measured for size in the unetched section and placed into size classes. The measurements are best performed by quantitative image analysis. The number of all measured pores is set equal to 100%. The material specifications for the respective spray coatings state the percentage of pores smaller than a specific value. An additional value is stated for the maximum size of individual pores. The specification further states the maximum pore size in the radial direction relative to the coating thickness.

1.9.4 Microstructure and Phase Distribution

The microstructure and the phase distribution of spray coatings are assessed on the etched micro-section. As these variables are difficult to quantify, the evaluation is performed by means of comparison against a classification chart for the spray coating concerned. The photomicrographs contained in the specifications represent only „averages“.

1.9.5 Unmelted Particles and Reaction Products

As a result of the spray process, plasma and flame sprayed coatings contain unmelted or only partially melted spray particles as well as reaction products usually of an oxidic nature.

Unmelted particles are recognizable as more or less round inclusions in the coating structure; reaction products can be present as thin layers between the coating lamellae. The permissible size and number of unmelted particles per sectional area is stated. The permissible shape and amount of reaction products is defined with the aid of reference micrographs (classification chart).

In the case of HVOF sprayed coatings it is the specific aim not to melt the spray powder but rather to compact the softened particles. Therefore unmelted particles in HVOF spray coatings are not a negative quality characteristic.

1.9.6 Micro-cracks and Fissures

Micro-cracks in the structure of spray coatings are short cracks discernible at 100x or greater magnification running between the coating lamellae or transversely across them. Fissures are lengthy cracks within fairly large coating areas or between the coating and the substrate metal.

The evaluation of spray coatings for microcracks and fissures is carried out on the unetched microsection. Microcracks are allowable, fissures are not.

Note: A ghost line at the coating to base material interface may be caused by relief formation during specimen preparation and will prevent a clear evaluation of the adhesion of the coating to the base material. If there is any doubt, the section must be suitably illuminated at an angle or an SEM micrograph taken in order to discriminate between a ghost line and a genuine fissure.

1.9.7 Coating Hardness

The coating hardness is measured according to Vickers as defined in DIN ISO 4516 and is stated as the average of 10 useful individual measurements per ring. The average must lie within the tolerance stated in the appropriate coating specification.

1.9.8 Particle and Phase Hardness

The hardness of individual particles and phases is measured on the etched section usually with HV 0.05. For very small particles and narrow phases it may be necessary to use a lower test force. In accordance with DIN ISO 4516 the test force is applied with an impact velocity of the indentor onto the specimen of 15-70 µm/sec. The equipment setting must not be altered for the duration of the test. The test force is allowed to act for 10 to 15 sec during which time no jolts or vibrations must be permitted to interfere with the applied force.

The average of 10 useful indentations is taken for each phase. The averages must lie within the tolerances stated in the specification.

1.9.9 Running Face Porosity, Voids, Cracks, Bond Defects between Coating and Inlay Groove Land (on Inlaid Rings)

These features, distinguishable on the running face, are influenced by the coating quality and above all by the machining. Such running face defects are tested by visual inspection, if appropriate with magnification. Guide values are laid down in DIN ISO 6621-5 for the evaluation of porosity and voids in the running face and for assessment of the running face edges and the outer edges at the ring gap. Macroscopic cracks in the running face are not permissible. If there is any doubt, a decision is made based on a suitable crack testing procedure. There must be no bond defects visible on the running face in the form of fissures between the coating and inlay groove land. However, allowance must be made for the occurrence of a partly discontinuous bond as a result of the unavoidably greater porosity of the coating structure caused by turbulence in the spray jet in the inlay groove wall region.

1.9.10 Coating Thickness

The thickness of spray coatings is determined with a device for measuring non-ferromagnetic coatings on ferromagnetic base materials (e.g. Permaskop). Standard reference values for different ring designs (full- face sprayed or inlaid) are obtained based on microscopic coating thickness measurements on radial cross- sections. The coating thickness is measured in the middle of the coating at three points around the ring circumference in accordance with DIN ISO 6621-2 and -4. The measured values must correspond to the drawing specification, with permissible tolerances stated in DIN

ISO 6621-5. The piston rings must be sufficiently demagnetized prior to measuring. If there is any doubt, the coating thickness must be determined on the radial cross-section.

1.10. Types of wear of the coating:

The study of the processes of wear of coating is part of the discipline of Tribology. The complex nature of coating wear has delayed its investigations and resulted in isolated studies towards specific wear mechanisms or processes. Some commonly referred to wear mechanisms of coating (or processes) include [59]:

1. Adhesive wear ,
2. Abrasive wear
3. Surface fatigue
4. Fretting wear
5. Erosive wear

A number of different wear phenomena of coating are also commonly encountered and represented in literature. Impact wear, cavitations wear, diffusive wear and corrosive wear are all such examples. These wear mechanisms; however, do not necessarily act independently in many applications. Wear mechanisms of the coatings are not mutually exclusive. "Industrial Wear" is the term used to describe the incidence of multiple wear mechanisms occurring in unison. Wear mechanisms and/or sub-mechanisms frequently

overlap and occur in a synergistic manner, producing a greater rate of wear than the sum of the individual wear mechanisms.

1.10.1. Adhesive wear of coating:

Adhesive wear is defined as the transfer of material from one surface to another during relative motion by a process of solid-phase welding or as a result of localized bonding between contacting surfaces. Particles that are removed from one surface are either permanently or temporarily attached to the other surface [29]. Adhesive wear of coating occurs when two body slides over each other, or are pressed into one another, which promote material transfer between the two surfaces. When either one of two surfaces of tribo-elements in sliding or rolling contact has thin soft surface layer that can partly transfer to the counter surface by adhesion, relative displacement takes place at the interface between the surfaces of coating and transfer layer with smaller shear strength of the soft material than that of the underlying element material. Low friction is obtained as a result, and wear of the tribo elements is much reduced. Soft metal coating is introduced for this purpose, and Au, Ag, Pb and In are representative ones [30]. However, material transfer in coating is always present when two surfaces are aligned against each other for a certain amount of time and the cause for material transfer or wear-categorization have been a source for discussion and argumentation amongst researchers for quite some time and there are frequent misinterpretations or misunderstandings due to overlaps and symbiotic relations between "wear" and physical-chemical mechanisms as previously mentioned. Having described the

restriction on the subject wear, we can focus on what causes material transfer in wear of coating.

Adhesive wear of the coating can be described as plastic deformation of very small fragments within the surface layer when two surfaces slides against each other. The asperities (i.e., microscopic high points) found on the mating surfaces will penetrate the opposing surface and develop a plastic zone around the penetrating asperity [31].

Dependent on the surface roughness and depth of penetration will the asperity cause damage on the oxide surface layer or even the underlying bulk material of the coating surface. In initial asperity/asperity contact, fragments of coating are pulled off and adhere to the other, due to the strong adhesive forces between atoms. It is thereby clear that physical-chemical adhesive interaction between the surfaces plays a role in the initial build-up process but the energy absorbed in plastic deformation and relative movement is the main cause for material transfer and wear of the coating.

Adhesive wear is the most common form of wear of coating and is commonly encountered in conjunction with lubricant failures. In engineering science, some aspects of adhesive wear is commonly referred to as welding wear due to the exhibited surface characteristics and the Tribology process is usually referred to as galling and is a common fault factor in sheet metal forming (SMF) and other industrial applications.

The tendency of contacting coating to adhere arises from the attractive forces that exist between the surface atoms of the two materials. The type and mechanism of attraction varies between different materials. Most solids will adhere on contact to some extent,

however, oxidation films and contaminants naturally occurring; generally suppress adhesion. Surfaces also generally have low energy states due to reacted and absorbed species. The mechanism of adhesive wear of coating occurs due to contact possibly producing surface plastic flow, scraping off soft surface films or breaking up and removing oxide layers. This brings clean regions into contact and introduces the possibility of strong adhesion. The removal of material from coating surface, or wear, takes the form of small particles. These small particles are usually transferred to the other surface but may come off in loose form.

1.10.2. Abrasive wears of coating:

The abrasive wear of a material is defined as the progressive loss of material due to abrasive action of hard particles present between the counter surfaces. The abrasive wear depends on various factors like abrasive size, rake angle of abrasives, applied load and shape, size, volume fraction of the dispersed phases. In addition to these factors the abrasive wear rate of a material also depends on the surface hardness and materials properties like fracture toughness [32]. Abrasive wear of coating occurs when a hard rough surface slides across a softer surface. ASTM (American Society for Testing and Materials) defines it as the loss of material due to hard particles or hard protuberances that are forced against and move along a solid surface. Abrasive wear of coating is commonly classified according to the type of contact and the contact environment. The type of contact determines the mode of abrasive wear of coating. The two modes of abrasive wear of coating are known as two-body and three-body abrasive wear. Two-body wear occurs when the grits, or hard particles, are rigidly mounted or

adhere to a surface, when they remove the material from the surface of coating [33]. The common analogy is that of material being removed with sand paper. Three-body wear occurs when the particles are not constrained, and are free to roll and slide down a surface of coating. The contact environment determines whether the wear is classified as open or closed. An open contact environment occurs when the surfaces are sufficiently displaced to be independent of one another.

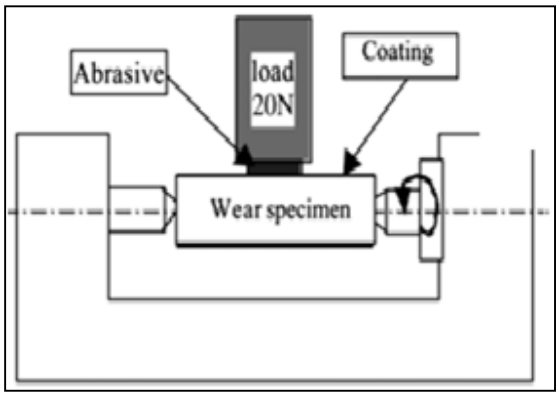

Figure 1.9 Abrasive wear of thermal spray coating (Reference 33)

There are a number of factors which influence abrasive wear of coating and hence the manner of material removal. Several different mechanisms have been proposed to describe the manner in which the material is removed. Three commonly identified mechanisms of abrasive wear of coatings are:

1. Plowing
2. Cutting
3. Fragmentation

Plowing occurs when coating material is displaced to the side, away from the wear particles, resulting in the formation of grooves that do not involve direct material removal from the coating surface. The displaced material forms ridges adjacent to grooves, which may be removed by subsequent passage of abrasive particles. Cutting occurs when coating material is separated from the surface in the form of primary debris, or microchips, with little or no material displaced to the sides of the grooves. This mechanism closely resembles conventional machining. Fragmentation occurs when material is separated from a surface by a cutting process and the indenting abrasive causes localized fracture of the coating material. These cracks then freely propagate locally around the wear groove, resulting in additional material removal by spalling.

1.10.3. Surface fatigue wear of the coating:

Surface fatigue wear of the coating is a process by which the surface of coating is weakened by cyclic loading, which is one type of general material fatigue. Fatigue wear in coating is produced when the wear particles are detached by cyclic crack growth of micro cracks on the surface of the coating. These micro cracks are either superficial cracks or subsurface cracks. It is extremely important to improve the resistance of the material against fracture in aerospace applications.

In the case where this alloy is, for example, used for turbine engine blades, the fretting fatigue, which is caused by the combination of cyclic fatigue stress and frictional wear, occurs at turbine engine blade roots. As a result, many small cracks will easily initiate on the material surface. Also, it has been reported that the fretting fatigue life decreases remarkably as compared with plain fatigue life [34]. The use of high strength steels

instead of tool steels brought out a new aims for material scientists – increase endurance of the tool materials in cyclic loading (cold forging, stamping and blanking). To solve the fatigue damage problems of high-speed steels (HSS) the powder metallurgy (PM) routes are used. As a result of the finer and more uniform microstructure that PM-HSSs exhibit, as compared to their conventionally produced counterparts, they also present enhanced cross-sectional hardness uniformity (wear resistance), fracture toughness and fatigue strength [35].

1.10.4. Fretting wear of coating:

Fretting wear of the coating is the repeated cyclical rubbing between coating and another surface, which is known as fretting, over a period of time which will remove material from one or both surfaces in contact. It occurs typically in bearings, although most bearings have their surfaces hardened to resist the problem. Another problem occurs when cracks in either surface are created, known as fretting fatigue [35]. It is the more serious of the two phenomena because it can lead to catastrophic failure of the bearing. It is extremely important to improve the resistance of the material against fracture in aerospace applications. In the case where this alloy is, for example, used for turbine engine blades, the fretting fatigue, which is caused by the combination of cyclic fatigue stress and frictional wear, occurs at turbine engine blade roots [36]. As a result, many small cracks will easily initiate on the material surface. An associated problem occurs when the small particles removed by wear are oxidized in air. The oxides are usually harder than the underlying metal, so wear accelerates as the harder particles abrade the metal surfaces further. Fretting corrosion acts in the same way, especially

when water is present. Torsional fretting wear tests of the coating were conducted on a flat-on-ball contact on a torsional fretting rig with a controlled environmental chamber.

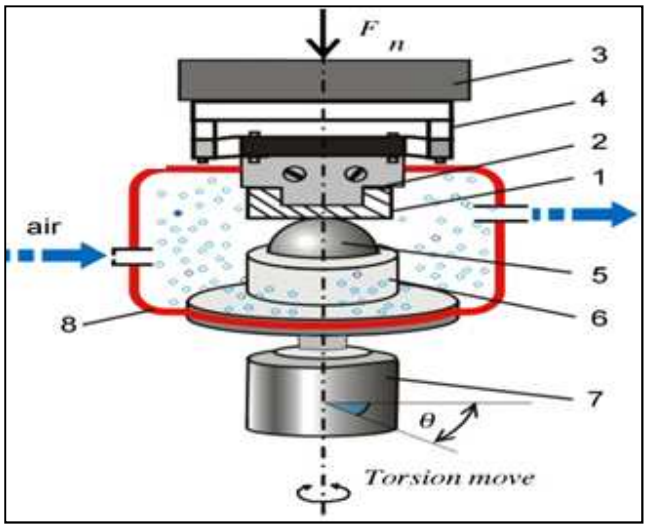

Figure 1. 10 Fretting wear of thermal spray coating (Reference 8)

A plate specimen (1) was fixed on the upper holder (2) to link a six-axis torque/force sensor (3) (three loads of *x*, *y* and *z* direction; three torques of *x*, *y* and *z* direction) through a spring suspension (4). A ball specimen (5) was mounted on the lower holder (6), which fixed on the low-speed reciprocating rotary motor system (7). The flat specimen rotated following the motion of the motor at a constant rotary velocity (in the range of 0.01–5◦/s). In order to ensure pure torsional fretting, the centerline the ball specimen was superposed strictly to the rotary axis of the motor system at all times [8]. Angular displacement of the contact pair was measured by a sensor in the motor system and unprotected bearings on large structures like bridges can suffer serious degradation in behaviour, especially when salt is used during winter to deice the highways carried by the bridges. The problem of fretting corrosion was involved in the Silver Bridge tragedy and the Mianus River Bridge accident.

1.10.5. Erosive wear of coating:

Erosive wear of the thermal spray coating is caused by the impact of particles of solid or liquid against the surface of coating [13]. The impacting particles gradually remove material from the coating surface through repeated deformations and cutting actions. It is a widely encountered mechanism in industry. A common example is the erosive wear associated with the movement of slurries through piping and pumping equipment (fig 1.11).

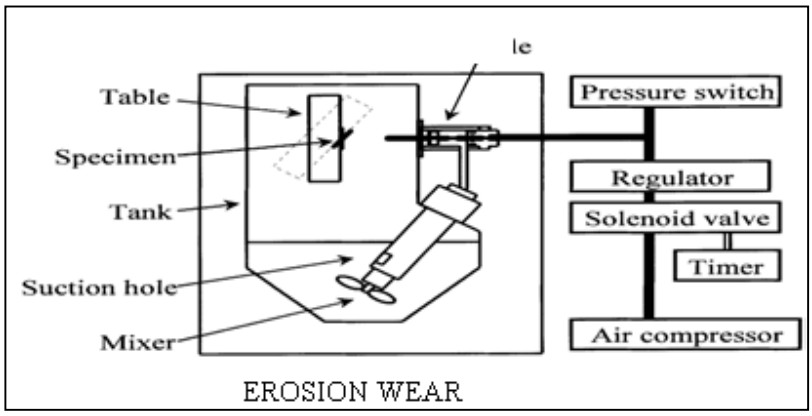

Figure 1.11 Erosion wear of thermal spray coating [13]

The rate of erosive wear is dependent upon a number of factors. The material characteristics of the particles, such as their shape, hardness, and impact velocity and impingement angle are primary factors along with the properties of the surface of the coating [13,28]. The impingement angle is one of the most important factors and is widely recognized in literature. For ductile coating materials the maximum wear rate is found when the impingement angle is approximately 30°, whilst for non ductile coating

materials the maximum wear rate occurs when the impingement angle is normal to the surface.

2.0 Testing on the Piston Rings

The various type of testing performed on the piston rings is to provide the best quality of piston rings, so that performance of the IC Engine can be increased as much as possible. Some of testing which are used on the piston rings from the starting (casting of rings) to the final product is mentioned below,

2.1 Microstructure Testing

The microstructure of the coating was studied under the optical microscope. To study the microstructure a piece of the track of coating was cut and then fixed in the thermosetting plastic to hold it. The fixing of the small piece of the coating piece was done on the automatic mounting press as described earlier in micro hardness test. The cross section of worn surfaces was analyzed, when the pin was sliding over the coating material there was a generation of heat which might result in change in the microstructure. It is known that the melting point of the aluminum is 662˚C [1] and when there is rise in temperature above recrystalisation temperature then there occurs a change in the microstructure. [4].

2.2 Chemical Composition Testing (using SEM/XRD/EDS)

Energy dispersive spectroscopy (EDS)

After 12 months of exposure, the 25*25*280 mm specimens used for the expansion test were also used for chemical analysis using quantitative Energy Dispersive Spectroscopy (EDS). Thin 25*25*10 mm samples were cut from original specimens exposed to sodium sulfate solution as shown in Fig. 4. These samples were polished

using 300 and 600 grit polishing papers and the 25*25 mm cross sections were marked using a sharp tipped pencil to generate a grid mesh as schematically shown in Fig. 5. The exterior layer is hereby called EXT and the interior portion is called INT for comparison purposes. A novel SEM-EDS setup was used and the quantitative compositional analyses of exposed samples were obtained using window scanning option with an area of 1 mm2 for each grid point.

2.3 Mechanical Strength (Micro Hardness)

The 25*25*10 mm thin specimens used for EDS were also used for micro-hardness testing to understand the mechanical changes on the exposed samples. Micro-indentation is a common method of evaluating the quality of materials for engineering purposes, in particular ductile materials (i.e. metals) but also brittle materials such as concrete [27,28]. This technique is based on applying a static load for a known period of time and measuring the response in terms of size of indentation. The Vickers hardness HV (GPa) is calculated per Eq. (6) in which P (Kgf) is the applied force, a is the indenter diagonals angle equal to 136 and D (mm) is the average of diagonals of the indentation [29, 30] In this study, a 0.2 Kgf load was applied on the samples for 15 s, followed by a measurement of indentation size using an optical microscope. For each grid point, three replicate indentations were made as shown in Fig. 6a and the average values were used for calculating the hardness values. Fig. 6b shows an SEM image of the indentation performed on a cement paste sample

2.4 Adhesion Testing

The adhesion strength of coatings deposited plasma arc spray (H_2 or N_2 as carrier gas) was tested. The thermally sprayed coatings were deposited in accordance with the recommendations of our experiment design, with the exception of the large splat coatings, where the parameters were slightly altered. The deposition parameters used in the plasma arc spray process are mentioned in the table XXXX. The coatings and their chemical compositions can be seen fromTable 1. Metcoloy 2 (wire) and Metco 3007 (powder) are standard products manufactured by Sulzer Metco. The size grades for the powder used with plasma arc spray process were 50 µm, respectively. The thicknesses of the coatings were in the range 1.5-2.5 mm for arc spray and 205 µm for the hard chrome plating. As substrate, piston rings made up of cast iron , were chosen. The surface roughness of the arc sprayed and hard chrome deposited substrate 3-4mm & 8-10mm, respectively (Ra-values). The Metcoloy 2 and 80Ni20Al materials were supplied as the two separate electrodes in the arc spray process, resulting in a coating consisting of 50% of each material. Two different arc spray droplet sizes, 50 and 200 mm, were examined for the Metcoloy 2q 80Ni20Al-coating.The adhesion of the coatings to the substrate was tested with the methods as described with the simple bending equipment as described below [76].

2.5 Wear testing on the piston rings Coatings

2.5.1 Types of wear test of piston rings coating:

Wear behavior of the can be measured on the different test and is mainly depends on the application of the coating and thickness of the coating. The test is carried out at

different wear conditions and the parameter are taken into consideration on which the wear is mainly depends. These tests are such mainly divided into these categories:

2.5.2 Scratch test of piston rings coating:

The scratch tester is used to test the scratch resistance of flat solid surfaces such as coatings, metals, ceramics, composites, polymers, and other material surfaces. The test is performed by sliding a stylus over the surface of the test specimen. The normal load, sliding speed, direction, stylus geometry, and stylus material can be varied. The resultant tangential force at the contact interface can be monitored using tribodata, the supplied windows-based data acquisition Software. The onset of scratch or adhesion failure of coatings can be inferred from this data. A CMOS camera is built-in to capture the scratch scar image. (Y. Xie et al. Y. Xie, H.M. Hawthorne, 1999) was investigated scratching an alumina coating, using conical diamond indenters with different tip radii under either progressively increasing or constant loading. The interaction between the coating and the indenter was studied by performing single scratching on a polished virgin surface, repeated scratching over the same track and closely-spaced, multiple parallel interacting scratching.

2.5.3 Slurry Abrasion Test of piston rings coating:

The Slurry Abrasion Tester is used to test the abrasive resistance of solid materials to slurry compositions. Slurry erosion problems are especially important during rainy seasons in hydroelectric power plants due to the increase in the number of solid particles impacting the surfaces, especially in systems where the installation of an exhaustive filtration process is not possible [83]. Various materials such as metals,

minerals, polymers, composites, ceramics, coatings, and heat-treated materials can be tested with this instrument. The test is performed by rotating a rectangular test sample within a cup filled with abrasive slurry (figure 2.1). The mass of the test sample is recorded before and after conducting a test and the difference between the two values is the resultant mass loss due to slurry abrasion [84].

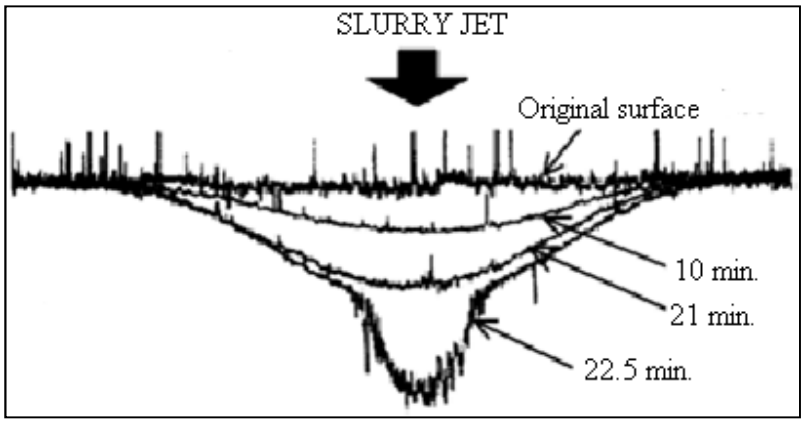

Figure 2.1 Slurry abrasion wears of thermal spray coating

To develop a comparison table for ranking different materials with respect to each other, it is necessary to convert this mass loss to volume loss to account for the differences in material densities. The test speed, temperature, duration, as well as test sample size and slurry composition, can be varied. The instrument is configured to run up to six test samples simultaneously at the same speed. The test temperature is maintained by immersing the slurry vessels in a water bath.

2.5.4 Friction Test of Physical Vapor Deposition coating:

The Friction Tester is used to test the frictional characteristics of materials in dry or lubricated reciprocating motion contact. A wide variety of materials including fluid

lubricants, greases, cutting fluids, metals, composites, ceramics, polymers, and coatings can be tested. The test is performed by loading the test specimen against a ball, pin, or cylinder undergoing reciprocating linear motion. The frictional force developed at the contact interface is measured by a force transducer. The output signal can be captured by a storage oscilloscope or tribodata, Koehler's data acquisition software, for evaluation. The reciprocating motion of the ball results in a unique velocity profile which allows for monitoring of static and dynamic friction force over a wide range of linear sliding speeds. The test load, stroke, frequency, and temperature can be adjusted to simulate different testing conditions. Wear testing may also be performed on the test specimen by evaluating the resulting wear scar with a profilometer. Yucong Wang et al. (Yucong Wang, Simon, Tung, 1999) were performed with a modified Cameron Plint reciprocating machine to determine the scuffing and wear behavior of piston coatings against 390 Al engine cylinder bore. The tested piston coatings included nickel–tungsten (Ni–W).plating, electro less Ni plating, Ni–P coatings with ceramic particles such as boron nitride (BN), Sic, as well as titanium nitride physical vapor deposition (PVD) coating, diamond-like carbon (DLC) coating, and hard anodizing.

2.5.5 Air Jet Erosion Test of Physical Vapor Deposition coating:

The Air Jet Erosion Tester is used to test the erosion resistance of solid materials to a stream of gas containing abrasive particulate. The test is performed by propelling a stream of abrasive particulate gas through a small nozzle of known orifice diameter toward the test sample. Material loss, in this case, is achieved via the impingement of small abrasive particles upon the surface of the test sample. Materials such as metals,

ceramics, minerals, polymers, composites, abrasives, and coatings can be tested with this instrument [84]. The test specimen, temperature, angle of incidence of the jet stream, abrasive particulate speed and flux density, can be varied to best simulate actual conditions. Special adapters are available to test various geometries and components for user-specified testing applications.

2.5.6 Pin on Disc Test of Physical Vapor Deposition coating:

The Pin-On-Disc Tester is used to test the friction and wear characteristics of dry or lubricated sliding contact of a wide variety of materials including metals, polymers, composites, ceramics, lubricants, cutting fluids, abrasive slurries, coatings, and heat-treated samples. The test is performed by rotating a counter-face test disc against a stationary test specimen pin (figure 2.2). The advantage of a wear test, when compared to indentation or scratch testing, is that it can give a measure of the lifetime of a particular coating-substrate system. In many applications of coatings, the resistance to wear can be more important than the load required to permanently damaging the material [86]. A spherical ended pin has the advantage that contact conditions can be relatively well controlled. No matter the degree of misalignment between pin axis and disk axis the initial apparent area of contact should be the same, for a given load. However, the apparent area of contact will then change during the test up to the maximum given by the pin-diameter Garcia-Prieto, M.D. Faulkner, J.R. Alcock, 2004. The pin on disc test can be used for a variety of coatings it may be thick or thin and can be made of any material such as metals, ceramics, cermets and composites (Binshi Xua, Zixin Zhua, Shining Maa, and Wei Zhang, Weimin Liu2004, , Y. Iwai a, T. Honda,

H. Yamadaa, T. Matsubara, M. Larsson, S. Hogmarkd 2001, Jeffree, C. E.; Read, Ambient- and Low-temperature scanning electron microscopy, Electron Microscopy of Plant Cells, London: Academic Press. pp. 313–413. ISBN 0123188806, Karnovsky, A formaldehyde-glutaraldehyde fixative of high osmolality for use in electron microscopy, Journal of Cell Biology 27: 137A).

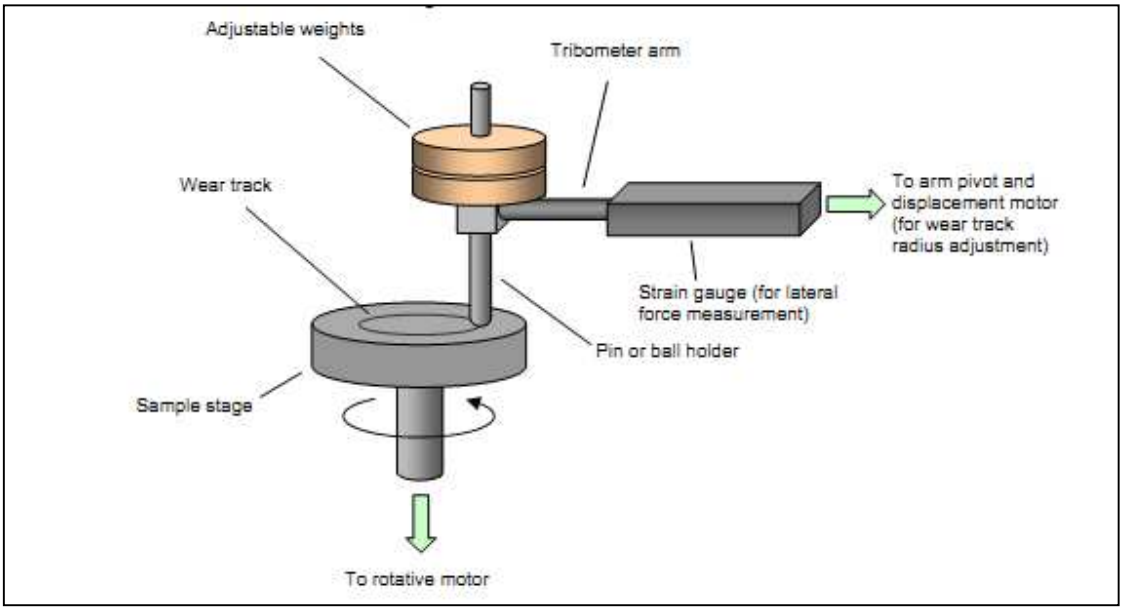

Figure 2.2 Pin on disc wear test of thermal spray coating (Reference 40)

There are various wear measurement methods available for assessing changes in the tribological system in terms of wear behaviour. Depending on the method used data can be obtained on mass wear, volumetric, localized or integral wear behaviour, and wear forms. All these methods are legitimate for particular problems but differ greatly in complexity

For high wear rates, the wear volume can be determined from macro geometrical changes or mass loss. In addition to sliding wear, surface degradation of piston rings

can take place due to blow-by of hot gases from the combustion chamber, where the temperature of the combustion gas is in the excess of 2 000℃. The blow-by can cause local melting or hot gas erosion damages, or burn scars, on the rings. In engines where ring deterioration owing to blow-by is likely to occur, the use of molybdenum or similar heat-resistant coatings is essential [91].

Besides the established PVD coatings for the wear protection of machining tools, this paper deals with coating development and model wear test results from PVD coatings on piston rings for combustion engines. Piston rings are examples for the application of thin films on commonly used mechanical components. The PVD Cr_xN coatings are deposited by RF magnetron sputtering and characterized by their fundamental mechanical properties like thickness, hardness, residual stress and adhesion, which are important for the tribological behaviour of the coating substrate compound. The contact mechanics of the tribological system piston-ring–cylinder are determined by high mechanical loading and changing geometry caused by the sliding kinematics. Therefore, the range of thickness is about 7 mm. The selected rings are made of steel DIN 1.4112 (DIN X 90CrMoV18) with a bore diameter of 97.5 mm. The results of the coating substrate characterization — high hardness, moderate compressive residual stresses and sufficient adhesion on metallic substrates — provide good behaviour of coatings in this tribological application. This is confirmed by the results of the tribological test procedures which have been performed with ring-on-disc model-wear tests and a short-stroke test rig [92].

The wear of piston rings and cylinder liners can be accelerated by three-body abrasive wear caused by minor abrasive particles in the lubricating oil. The contaminant particles

causing the three-body abrasive wear can originate from the oil sump or from the combustion chamber. In addition to the two-body and three-body abrasive wear, the overall wear rate can be tribochemically accelerated by aggressive components in the lubricant that have been entrapped in the ring zone. Aggressive combustion products are formed in particular when highly sulphuric fuels are used. Concerning most tribological applications, literature on the influence of the tribochemical wear on the overall wear of piston rings is only available to a rather limited extent. Experiences of chromium plated piston rings show that they offer good protection against wear caused by acidic combustion products [93].

Under conditions of poor lubrication, strong adhesive forces between the piston rings and cylinder liner may occur, leading to piston ring scuffing that comprises high friction forces and the formation of severe wear scars on the piston, ring and cylinder surfaces. As presented by Coy in his qualitative wear transition model, conditions of hydrodynamic lubrication at the mid-stroke region of the piston motion give rise to full film lubrication ($\lambda > 5$) and zero wear, while sliding under less favorable conditions in the vicinity of the dead centers of the piston motion cause mixed lubrication ($\lambda = 1...5$) and wear inversely proportional to the oil film thickness [94].

For low wear rates, the wear volume of piston rings can be determined by comparison of surface roughness profiles or cross section profiles before and after the tests (Shuster et al., 1999). Alternatively, the wear can be estimated from changes in relevant surface roughness parameters representing certain proportions of the piston ring face surface area [95].

It is commonly assumed that the wear of piston rings proceeds according to a mild mechanism of mild two-body abrasive wear against the cylinder liner, expressed by the formulae presented by Archard, Archard and Hirst, Preston, Rabinowitcz or Holm, while in reality the wear process is significantly more complicated[96].

The wear interaction between piston ring and piston groove in a radial piston hydraulic motor was studied in regard to mass loss and changes in form and surface roughness. A specially developed test rig that simulates the tilting movements of pistons at the end of strokes was used in the test. The results show that wear on the piston ring groove can be up to 10 times greater than the wear on the piston ring. For both interacting surfaces, the dominant wear mechanism was mild wear [75].

Laboratory tests to evaluate piston ring and cylinder liner materials for their friction and wear behavior in realistic engine oils are described to support the development of new standard test methods. A ring segment was tested against a flat specimen of gray cast iron typical of cylinder liners. A wide range of lubricants including Jet A aviation fuel, mineral oil, and a new and engine-aged, fully formulated 15W40 heavy duty oil were used to evaluate the sensitivity of the tests to lubricant condition. Test temperatures ranged from 25 to 100 8C. A stepped load procedure was used to evaluate friction behavior using a run-in ring segment. At 100 8C, all lubricants showed boundary lubrication behavior, however, differences among the lubricants could be detected. Wear tests were carried out at 240 N for 6 h at 100 8C with new ring segments. The extent of wear was measured by weight loss, wear volume and wear depth using a geometric model that takes into account compound curvatures before and after testing.

Wear volume by weight loss compared well with profilometry. Laboratory test results are compared to engine wear rates [77].

Two new substoichiometric titania (TiOx) coatings designated for cylinder liner application were deposited on specimen of grey cast iron GG20HCN with high carbon content by plasma spraying. First, a TinO2n−1 coating was prepared by atmospheric plasma spraying (APS) using a sintered and agglomerated Magneli-type spray powder. Second a TiO ´ 1.95−x coating was deposited with a vacuum plasma spray (VPS) process using a commercial, fused and crushed TiO1.95 powder. The tribological behaviour of these coatings under lubricated conditions was compared with uncoated specimen of this grey cast iron. As counter bodies a widespread used APS-sprayed Mo-NiCrBSi piston ring coating (MKP81A®), an advanced HVOF-sprayed WC/Cr3C2-based (MKJet502®) ring coating as well as non-commercial prototype APS-sprayed TinO2n−1 and APS sprayed (Ti, Mo)(C,N) + 23NiMo (TM23-1) coatings were tribotested. The interaction of the pairs with prototype engine oils based on esters and polyglycols were studied under mixed/boundary lubrication using the BAM test method. Lubricants were factory fill engine oils, ester-containing lubricants with low-SAP (sulphur–ash–phosphor) and/or bio-notox properties as well as polyglycole-based lubricants. The ester and polyglycole-based engine oils respond both to bio-no-tox criteria and are polymer-free. They follow different strategies to reduce zinc, phosphorus and sulphur to assure low ash content. Both TiOx coatings designated for cylinder liners meet or exceed the wear resistance of the grey cast iron with high carbon content when paired with APS-sprayed TinO2n−1 or Mo-NiCrBSi piston ring coatings. Overall, in nearly all pairs the wear rates of the APS TinO2n−1 coating were lower than those of the VPS TiO1.95−x coating.In

order to characterize the tribological behaviour under oil-off, dry-running conditions, additional tests were performed under unlubricated unidirectional sliding conditions at 22 and 400 ^{0}C for a sliding speed of 1 m/s against sintered polycrystalline Al2O3 as stationary specimen [78].

The piston system accounts for roughly half of the mechanical friction of an internal combustion engine, thus it is important to optimize. Different thermally sprayed cylinder liners were investigated in order to optimize the frictional impact of the contact between cylinder liner and piston ring/piston. A novel tribometer test setup was used to scan through different materials at different running conditions. Two cylinder liner materials showed significantly lower friction than the other tested materials, CrC–NiCr and MMC. All the thermally sprayed cylinder liners were worn significantly less than the reference material. Based on these results a full-scale single cylinder test was performed to validate the results from the rig. Comparing the thermally sprayed cylinder liner MMC with reference cylinder liner the test showed higher friction torque for the MMC cylinder liner except in one case; at low speed and high pressure. An analysis of the results between the tribometer and the engine points at the importance of the ratio between viscous and mechanical friction losses. The most probable cause of higher friction torque for the thermally sprayed coating (MMC) is that the functional surface of the cylinder liner promotes an increase in viscous friction [79].

Published data on piston ring and cylinder bore wear in engines is very limited because of the technical difficulties involved in performing the measurements. Moreover, cylinder bore wear is more difficult to measure than ring wear because it occurs over a much larger surface area, and the wear rates vary widely at different locations on the bore. In

this paper, cylinder liner surface roughness and wear measurements were performed through an experimental study of a single cylinder diesel engine operating at a steady-state. A replication method was used to evaluate wear and surface roughness on a cylinder liner, where measurements were made at different locations on the cylinder liner before and after each test. Replicated surface profiles were measured by a WYKO NT 1100 optical surface profilometer. It was found that surface roughness decreased with time and the rate of decrease was higher during the run-in period. A unique wear volume calculation method that includes bearing ratio parameters was proposed, and reasonable results for wear volume were obtained. Cylinder bore wear rates measured by this replication method were consistent with long-term wear observed in different tests of diesel engines [80].

The piston system accounts for roughly half of the mechanical friction of an internal combustion engine, thus it is important to optimize. Different thermally sprayed cylinder liners were investigated in order to optimize the frictional impact of the contact between cylinder liner and piston ring/piston. A novel tribometer test setup was used to scan through different materials at different running conditions. Two cylinder liner materials showed significantly lower friction than the other tested materials, CrC–NiCr and MMC. All the thermally sprayed cylinder liners were worn significantly less than the reference material. Based on these results a full-scale single cylinder test was performed to validate the results from the rig. Comparing the thermally sprayed cylinder liner MMC with reference cylinder liner the test showed higher friction torque for the MMC cylinder liner except in one case; at low speed and high pressure. An analysis of the results between the tribometer and the engine points at the importance of the ratio between

viscous and mechanical friction losses. The most probable cause of higher friction torque for the thermally sprayed coating (MMC) is that the functional surface of the cylinder liner promotes an increase in viscous friction [81].

Plasma spray coating, hard chrome plating and gas nitriding on cast iron substrate were successfully prepared by three different processes. There are different thermal spray process such as combustion flame spray, high velocity oxy- fuel spray, plasma spraying , vacuum plasma spraying and cold sprays. But the coating produced by plasma arc spray process is widely used in the industries and the process is easy to control. The cast iron substrate was used because the coating after solidification will give the same result as piston cylinder assembly. After preparation of the coating the coating is cleaned. The coating was cut in the form of plate of 90X90X2 mm to control the weight of the disc with in the limit of 120 gram and fixture was designed to fix the plate on the tribometer with the help of screw and nut .There are different wear test such as scratch test, slurry abrasion test, erosion test and **pin on the disc test**. The selection of the wear test depends on the material of the coating and its applications. For marine applications of the coating slurry erosion and corrosion test are commonly perform. But in case of dry applications of the coating the pin on disc and scratch test are commonly perform. For the present study two variables were selected for wear test that was load (30, 40 and 50 N) and wear track (50,60 and 70mm) sliding distance(1.2km) remain fixed during the test. Wear test of the coating was conducted on pin on disc machine under dry conditions. The wear rate was calculated by mass loss methods. The wear disc was weigh before and after the wear test on an electronic balance having least count 0.0001g. The coefficient of friction was found with LVDT which give the frictional

force during wear test. The surfaces morphology of worn surfaces of the coating was analysed with scanning electron microscope. The XRD of the worn surfaces was done to determine the change in intermolecular spacing of the worn surfaces of the coating. The wear rate of the coating was found to be increased with increased in load as well as sliding speed. The co-efficient of friction of the coating was found to be decreased with increased load and sliding speed. The d-spacing of the coating molecules on the wear track was found to be decreased with increased in load during the wear test. The microstructure of the worn surfaces of the coating was also examined with optical microscope and no change in microstructure of the coating due to frictional heat was observed. The micro hardness at the cross section of the coating at the wear track was found to be decreased away from the wear track. The main wear mechanism examined by scanning electron was adhesion, deformation and Microcutting.

3. EXPERIMENTAL PROCEDURE:

3.1 Sample Preparation:

Casting is a manufacturing process by which a liquid material is usually poured into a mold, which contains a hollow cavity of the desired shape, and then allowed to solidify. The solidified part is also known as a casting, which is ejected or broken out of the mold to complete the process.

Rings is always produced in circular shape for the market use and it is very hard to get a fresh piston rings to produce in our desired shaped because lots of finishing operation is already performed on the rings material. As per our machine Pin on Disc tribometer either we have to produce a pin of circular shape or disc of desired dimension. In our experiment we decided to produce a disc of the well know composition for the testing purpose.

A wooden pattern of the desired dimension based on the constrained of the plasma spray coating machine is prepared, for the easy removal of the casting a draft of $½^{0}$ is provided on the pattern. A sand mould is prepared with the help of press and the cavity is ready for the pouring of metal.

Molten metal is prepared of with the pure constituent powder. The powder of **Carbon (C) , Silicon (Si) , Magnesium(Mn) , Phosphorous (P) , Sulphur (P) ,Chromium (Cr) & Copper (Cu)** are used for the preparation of charge for the furnace . For the

melting of this powder Induction Arc Furnace (Fig 3.1) is used at a temperature of 1540 ^{o} C.

Fig 3.1 Induction Arc Furnace Used for the Melting of Charge

Figure 3.2 Powder as charged (A) Mn Slab (B) Cu Powder (C) Si Powder (D) Cr Powder

The induction arc furnace is preferred because it provides uniform melting of the charge. Stag Casting is done for the preparation of the entire sample at one shot to get the uniform composition of the entire slab. The composition of the slab is controlled as per the following table-3.1

Element	C (%)	Si (%)	Mn (%)	P (%)	S (%)	Cr (%)	Cu (%)
Target	3.75±0.05	2.70±0.05	0.53±0.01	0.36±0.02	.06±0.005	0.04±0.01	0.035±0.03

Table-3.1- Composition of the test sample prepared

The composition of silicon can vary on the basis of inoculation. The composition of chromium & Sulphur is very strictly controlled.

During the casting we faced problem of mould leak several times. It's also very difficult to get the casting of 280 X 90 X 15 mm thickness without bending or distortion.

After the solidification of the casting it's removed from the mould by breaking the sand mould and the sand blasting operation using SiC powder is done to clean the casting. Now slab is prepared but with irregularities and poor surface. Grinding Operation is required for the accurate dimension and clear surface.

3.2. Coating Preparation:

Coating is a covering that is applied to the surface of an object, usually referred to as the substrate. In many cases coatings are applied to improve surface properties of the substrate, such as appearance, adhesion, weldability, corrosion resistance, wear resistance, and scratch resistance. In other cases, in particular in printing processes and semiconductor device fabrication (where the substrate is a wafer), the coating forms an essential part of the finished product.

3.2.1 Physical Vapor Deposition

Physical vapor deposition processes (often just called thin film processes) are atomistic deposition processes in which material is vaporized from a solid or liquid source in the form of atoms or molecules and transported in the form of a vapor through a vacuum or low pressure gaseous (or plasma) environment to the substrate, where it condenses. Typically, PVD processes are used to deposit films with thicknesses in the range of a few nanometers to thousands of nanometers; however, they can also be used to form multilayer coatings, graded composition deposits, very thick deposits, and freestanding structures. The substrates can range in size from very small to very large, for example the 10'X12' glass panels used for architectural glass. The substrates can range in shape from flat to complex geometries such as watchbands and tool bits. Typical PVD deposition rates are 10–100Å (1–10 nanometers) per second. Physical vapor deposition processes can be used to deposit films of elements and alloys as well as compounds using reactive deposition processes. In reactive deposition processes, compounds are

formed by the reaction of the depositing material with the ambient gas environment such as nitrogen (e.g. titanium nitride, TiN) or with a co-depositing material (e.g. titanium carbide, TiC). Quasi-reactive deposition is the deposition of films of a compound material from a compound source where loss of the more volatile species or less reactive species during the transport and condensation process is compensated for by having a partial pressure of reactive gas in the deposition environment; for example, the quasi-reactive sputter deposition of ITO (indium–tin oxide) from an ITO sputtering target using a partial pressure of oxygen in the plasma. The main categories of PVD processing are vacuum deposition (evaporation), sputter deposition, arc vapor deposition, and ion plating, as depicted in Figure 3.3

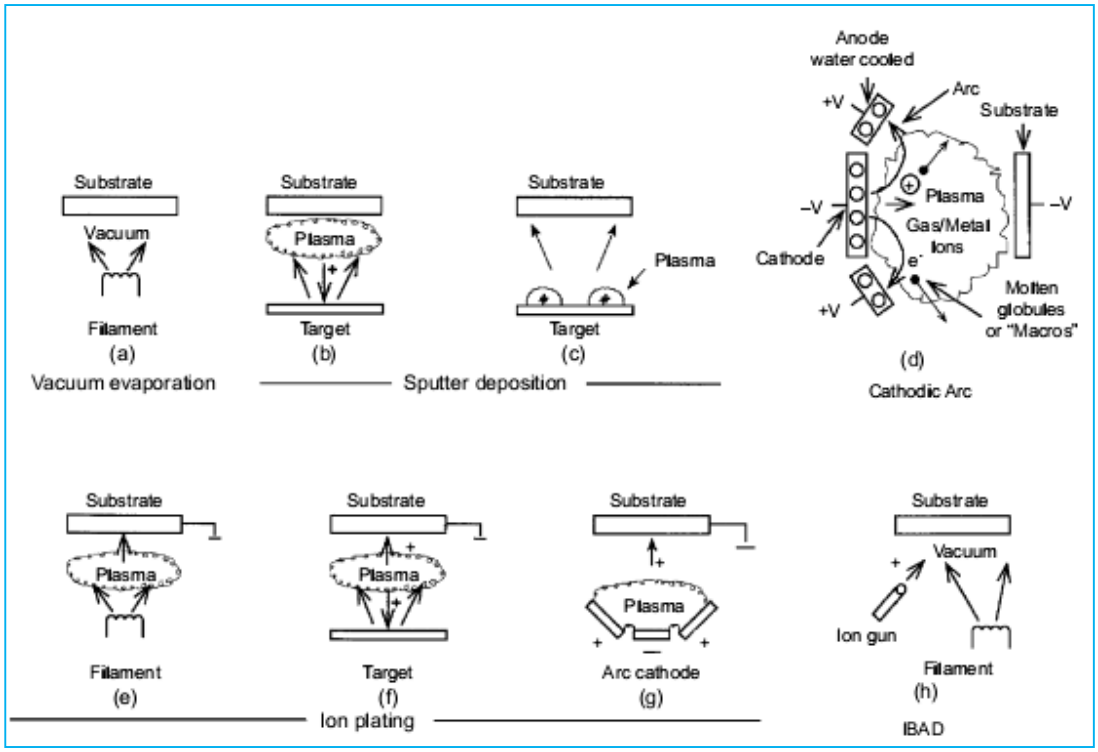

Figure3.3 : PVD Processing Technique (a) Vacuum Evaporation (b) & (c) Sputter Deposition in plasma environment (d) Sputter deposition in vacuum (e) Ion plating in plasma environment with a thermal evaporation source and (f) Ion plating with

sputtering source (g) Ion plating with an arc vaporization source and (h) Ion beam assisted deposition (IBAD) with a thermal evaporation source & Ion bombardment from an ion gun

3.2.2 Ion Plating:

Ion-plating is an atomistic deposition process that utilizes continuous or periodic bombardment of the substrate and depositing atoms of film material by atomic-sized energetic particles. The bombardment prior to deposition sputter cleans the surface. Bombardment during deposition is used to obtain good adhesion, densify the depositing material, aid in chemical reactions, modify residual stress, and otherwise modify the structure, morphology, and properties of the depositing film or coating. It is important, for best results, that the bombardment be continuous between the cleaning and the deposition portions of the process in order to maintain an atomically clean interface.

Ion-plating is also called ion-assisted deposition or ionization-assisted deposition (IAD), ion vapor deposition (IVD), ionized physical vapor deposition (IPVD, iPVD)[101], and energetic condensation.[102] This definition does not specify the source of the depositing film material, the source of the bombarding particles, nor the environment in which the deposition takes place. The concept and application of ion plating was first reported in the technical literature in 1964.[103] The technique was initially used for the improvement of adhesion and surface coverage as well as the densifying of PVD films. The technique was subsequently shown to enhance chemical reactions in the reactive deposition of compound thin films. Later it was shown that the concurrent bombardment could be used where the depositing atoms were from a chemical vapor precursor. The

bombardment was shown to control film properties such as density and residual film stress. An early review was written on the ion plating process in 1973.[104]

Often the term “ion plating” is accompanied by modifying terms – for example, “sputter ion plating”, “reactive ion plating”, “chemical ion plating”, “alternating ion plating”, “arc ion plating”, “vacuum ion plating”, etc. – which indicate the source of the depositing material, the method used to bombard the film, the deposition environment, or other particular conditions of the deposition. There are two common versions of the ion plating process. In “plasma-based ion plating”, typically a negatively biased substrate is in contact with plasma and bombarding positive ions are accelerated from the plasma and arrive at the surface with a spectrum of energies. In plasma-based ion plating, the substrate can be positioned in the plasma-generation region or in a remote or downstream location outside the active plasma-generation region. The substrate can be the cathode electrode in establishing a plasma in the system. Figure 3.4(a) shows a simple plasma-based ion plating configuration using a resistively heated vaporization source. In “vacuum-based ion plating”, the film material is deposited in a vacuum and the bombardment is from an ion source (“gun”). The first reference to vacuum-based ion plating or vacuum ion plating was in 1973,[105] when it was used to deposit carbon films using a carbon ion (“film ion”) beam.[106] In a vacuum, the source of vaporization and the source of energetic ions for bombardment may be separate. This process is often called ion beam-assisted deposition (IBAD).[107] Often, the ion beam is “neutralized” by the addition of electrons so the beam is volumetrically neutral . This prevents columbic repulsion in the beam and charge buildup on the bombarded surface. Figure 3.4(b) shows a simple vacuum-based (IBAD) system using an e-beam

evaporation source and an ion gun. In reactive ion plating, the plasma activates the reactive species, or reactive and inert ion species are produced in an ion source or plasma source. The bombardment enhances the chemical reactions and densifys the depositing film. The bombardment-enhanced interactions on the surface are complex and poorly understood.[108] In some cases, such as when using low voltage, high current e-beam evaporation, arc vaporization, high power pulse magnetron sputtering, or post-vaporization ionization, an appreciable portion of the vaporized film atoms is ionized to create “film ions”, which can also be used to bombard the substrate surface and growing film. The important parameters in non-reactive ion plating are the mass and energy distribution of the bombarding species, and the flux ratio of bombarding species to depositing atoms.[109,110]The flux ratio (ions : atoms) may be from 1 : 10 if energetic (>500 eV) ions are used to greater than 10 : 1 if low energy (<10eV) ions are used. Typically, it is found that above a certain energy level the flux ratio is more important in the modification of film properties than is the bombardment energy.

High energy bombardment can have differing effects from low energy bombardment. For example, low energy (~5 eV) bombardment promotes surface mobility of the ad atoms and is used to aid in epitaxial growth,[111] while high energy bombardment generally promotes the formation of a high nucleation density and a fine-grained deposit. The energy distribution of the bombarding species is dependent on the gas pressure, [112] so gas pressure control is an important

process parameter in plasma-based ion plating. In reactive ion plating, the chemical reactivity of the energetic bombarding and depositing species are important process parameters.

3.2.3 Stages of Ion plating

The ion plating process can be divided into several stages where the bombardment affects the film formation:

1. The substrate surface can be sputter cleaned or the surface “activated” in the deposition chamber.
2. Bombardment during the nucleation stage of film deposition can increase the nucleation density and cause recoil implantation of depositing film atoms into the substrate surface

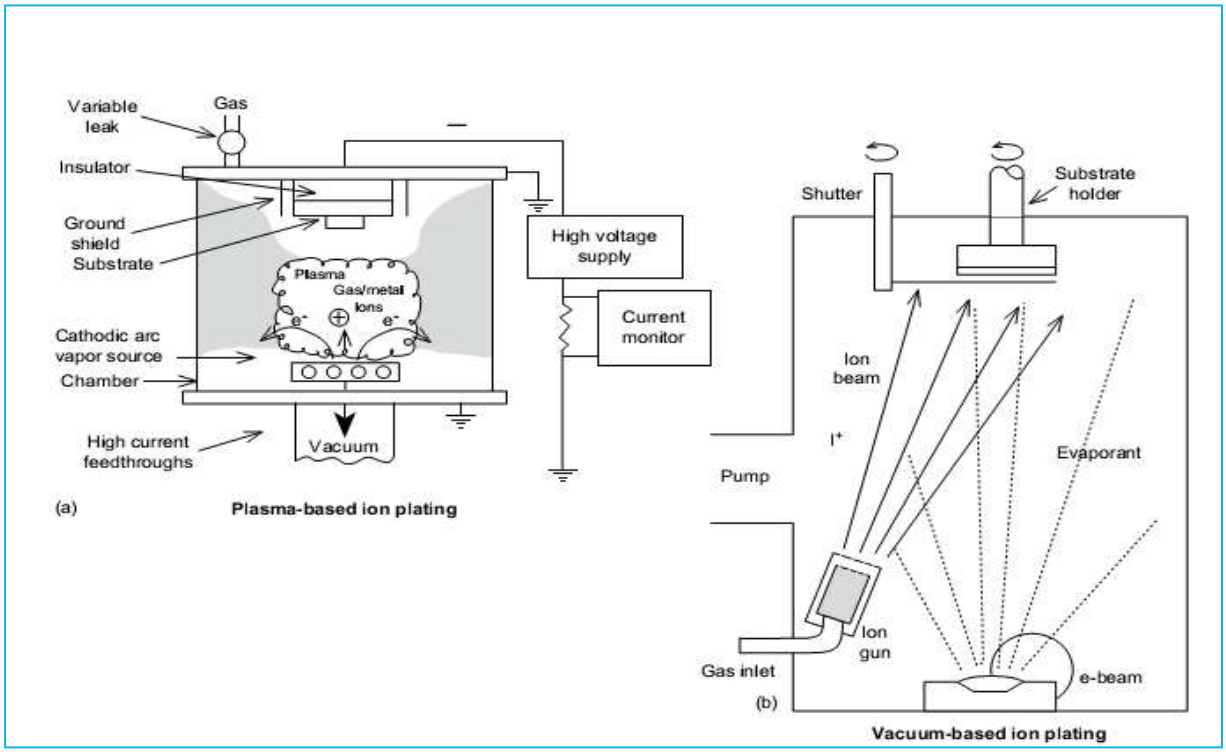

Figure3.4 -Ion Plating Configurations: (A) Plasma Based Ion Plating (B) Vacuum Based Ion Plating

3. Bombardment during interface formation adds thermal energy to the surface and introduces lattice defects into the surface region, which promotes diffusion and reaction.
4. Bombardment during film growth densifys the film, causes recoil displacement of near-surface atoms (atomic peening), causes sputtering and redeposition, and adds thermal energy.
5. In reactive deposition, bombardment aids chemical reactions on the surface and the presence of plasma activates reactive species. The bombardment may also preferentially remove un-reacted species from the growing deposit. It is important that the surface preparation stage blends into the deposition stage so that there will be no recontamination of the substrate surface after in situ surface cleaning and/or activation. In some cases, the high potential and bombarding flux used for surface preparation must be decreased during the nucleation stage in order to allow a film to form and not sputter away all of the depositing film atoms.

3.3 Design of Experiment:

Statistical methods are commonly used to improve the quality of a product or process. Such methods enable the user to define and study the effect of every single condition possible in an experiment where numerous factors (load and sliding speed) were involved in present work to study the wear behavior of the piston rings coatings. There were two parameters Load & Speed which were taken into consideration to determine the wear rate and coefficient of friction. There are several methods to design the experiment but we have chosen constant sliding distance (2 Km) with increasing RPM (550,650,750,850) with varying load of 40N, 50N, 60N & 70N (Table 3.10). To determine the response such as wear rate, coefficient of friction, microstructure, EDS analysis, and XRD analysis.

Variables	Level 1	Level 2	Level 3	Level 4
Sliding speed (rpm)	550 rpm	650 rpm	750 rpm	850 rpm
Load (kg)	4 kg	5 kg	6 kg	7 kg

Table 3.2 Variables for wear test

Coatings	Counter Body	Run	Load(N)	Sliding speed (rpm)
Ion Plating	WC,HCS,MS	1,1',1''	40	550
Ion Plating	WC,HCS,MS	2,2',2''	50	650
Ion Plating	WC,HCS,MS	3,3',3''	60	750
Ion Plating	WC,HCS,MS	4,4',4''	70	850

Table-3.3 Design of experiment table for wear test

3.4. Pin on disc test:

Pin on disc type wear monitor with data acquisition system was used to evaluate the wear behavior of aluminum alloys against three pin of WC Nickel & En-31. Load was applied on pin by dead weight through pulley string arrangement. The system had maximum loading capacity of 200 N. The test was performed under dry unlubricated condition. The wear test can be performed on any wear tester, but for thin coatings pin on disc wear test is most commonly used (figure 3.8).

Figure 3.5- Wear and friction monitor machine for pin on disc test

Figure 3.6 Ion Plated Disc before wear test

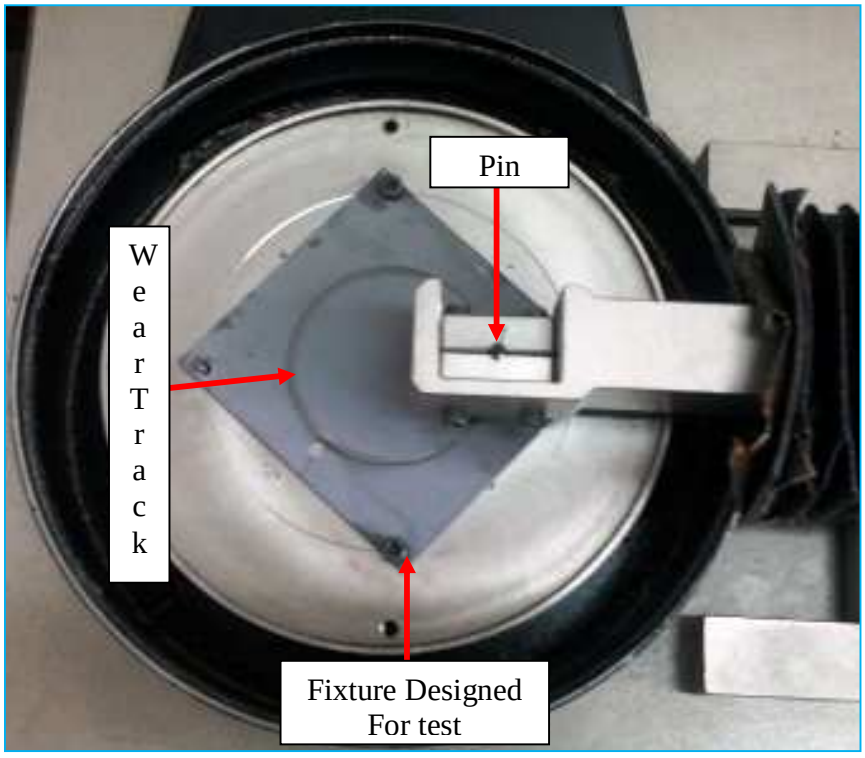

Figure 3.7 Ion Plated Disc during wear test

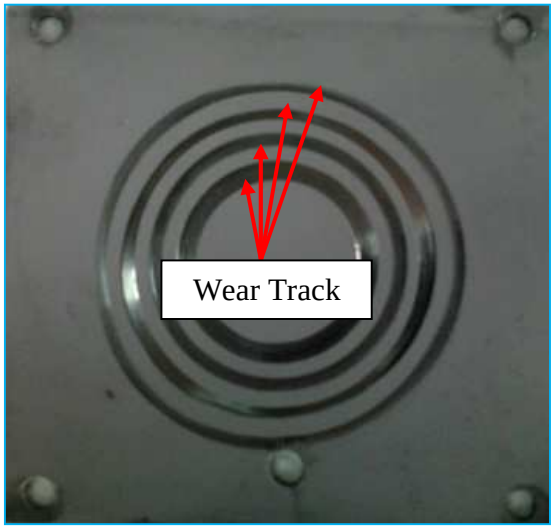

Figure 3.8 – Ion Plated Specimen after wear test

The machine is attached with the computer with software WINDCUM 2008. A window is open in the software and there are options to select various loads, times, pin diameter. The machine directly gives the coefficient of friction on the selected loading and sliding conditions. In this machine basically there is a rotating disc; and a pin is fixed over stainless steel pin holder. The pin can be loaded with different loads, it can be change externally. The coating pasted disc fastened on the machine with the help of screws (figure 3.9). The load was applied on the pin through dead weight loading arrangement. The coating surface and pin was initially washed with methyl alcohol so that, moisture should not present on coating surface. Initially, the brass pin was fixed on the pin holder; the wear rate of the coatings was calculated at different loading and sliding conditions. The wear rate was calculated by weighing the disc before after the wear test in terms of grams on an electronic balance of least count 0.00001g. The load was taken as 40, 50, 60 and 70 N respectively and the sliding speed was taken as 550 rpm, 650 rpm, 750 rpm, 850 rpm & distance was taken 2.0 km. The wear behaviour against three

various counter pin material was analyzed that was HCS, MS and WC pin. The pin of diameter 3 mm was chosen for all of the three materials. The wear test carried out at room temperature of 20˚C. During the wear test some amount of material also gets deposited on the pin in the form of a tribolayer so pin was cleaned after every test. So that there was always contact between pin and the coating surface, and the wear mechanism was between pin and coating surface, and a wear track was formed on the coating (figure 3.10)

3.5. Scanning electron microscope:

A scanning electron microscope (SEM) is a type of electron microscope that images a sample by scanning it with a high-energy beam of electrons in a raster scan pattern (figure 3.11). The electrons interact with the atoms that make up the sample producing signals that contain information about the sample's surface topography, composition, and other properties such as electrical conductivity.

Figure 3.9- Scanning electron microscope in DTU, Delhi

In a typical SEM, an electron beam is thermionically emitted from an electron gun fitted with a tungsten filament cathode. Tungsten is normally used in thermionic electron guns because it has the highest melting point and lowest vapour pressure of all metals, thereby allowing it to be heated for electron emission, and because of its low cost. For conventional imaging in the SEM, specimens must be electrically conductive, at least at the surface, and electrically grounded to prevent the accumulation of electrostatic charge at the surface. Metal objects require little special preparation for SEM except for cleaning and mounting on a specimen stub. Nonconductive specimens tend to charge when scanned by the electron beam, and especially in secondary electron imaging mode, this causes scanning faults and other image artifacts. They are therefore usually coated with an ultrathin coating of electrically-conducting material, commonly gold, deposited on the sample either by low vacuum sputter coating or by high vacuum

evaporation. Conductive materials in current use for specimen coating include gold, gold/palladium alloy, platinum, osmium, iridium, tungsten, chromium and graphite [47]. Coating prevents the accumulation of static electric charge on the specimen during electron irradiation. For SEM, a specimen is normally required to be completely dry, since the specimen chamber is at high vacuum. Hard, dry materials such as wood, bone, feathers, dried insects or shells can be examined with little further treatment, but living cells and tissues and whole, soft-bodied organisms usually require chemical fixation to preserve and stabilize their structure. Fixation is usually performed by incubation in a solution of a buffered chemical fixative, such as glutaraldehyde, sometimes in combination with formaldehyde [48-50]. In order to study the wear mechanism the worn surface were examined by scanning electron microscope of S-3700 series in DTU, Delhi. To see the microstructure of the wear track the coating material is coated with gold. Then it was put on job holder, the job holder was then moved inside the chamber of the scanning electron microscope. The scanning electron microscopy was used to determine the surface morphology of the wear track which gave the wear mechanism at various loading conditions and various speeds. For SEM of samples following parameters were chosen that were Accelerating Voltage=15000 Volt, Deceleration Voltage = 0 Volt, Magnification=1000, Working Distance=12600 um, Emission Current=80000 nA.

3.6. X -Ray diffractometer:

X ray diffractometer is a measuring instrument for analyzing the structure of a material from the scattering pattern produced when a beam of radiation or particles (as X rays or neutrons) interacts with it. A typical diffractometer consists of a source of radiation, a

monochromator to choose the wavelength, slits to adjust the shape of the beam, a sample and a detector (figure 3.12). In a more complicated apparatus also a Gonio meter can be used for fine adjustment of the sample and the detector positions. When an area detector is used to monitor the diffracted radiation a beam stop is usually needed to stop the intense primary beam that has not been diffracted by the sample. Otherwise the detector might be damaged. Usually the beam stop can be completely impenetrable to the X-rays or it may be semitransparent. The use of semitransparent beam stop allows the possibility to determine how much the sample absorbs the radiation using the intensity observed through the beam stop. The specimen of the worn surfaces was placed on X-ray chamber. The scanning of the specimen was done from angle 20˚ to 90˚ and the scanning speed was chosen as 2 degree/min.

Figure 3.10-X-Ray diffractometer in DTU, Delhi

3.7. Vickers micro hardness tester:

Vickers Hardness Tester is a key piece of equipment that is indispensable to metallographic research, product quality control, and the development of product certification materials.

Vickers Microhardness test procedure as per ASTM E-384, EN ISO 6507, and ASTM E-92 standard specifies making indentation with a range of loads using a diamond indenter which is then measured and converted to a hardness value. For this purpose as long as test samples are carefully and properly prepared, the Vickers Microhardness method is considered to be very useful for testing on a wide type of materials, including metals, composites, ceramics, or applications such as testing foils, measuring surface of a part, testing individual microstructures, or measuring the depth of case hardening by sectioning a part and making a series of indentations. Two types of indenters are generally used for the Vickers test family, a square base pyramid shaped diamond for testing in a Vickers hardness tester and a narrow rhombus shaped indenter for a Knoop hardness tester.

The Vickers hardness test method requires a pyramidal diamond with square base having an angle of 136° between the opposite faces. Upon completion of indentation, the two diagonals will be measured and the average value will be considered (figure 3.13).

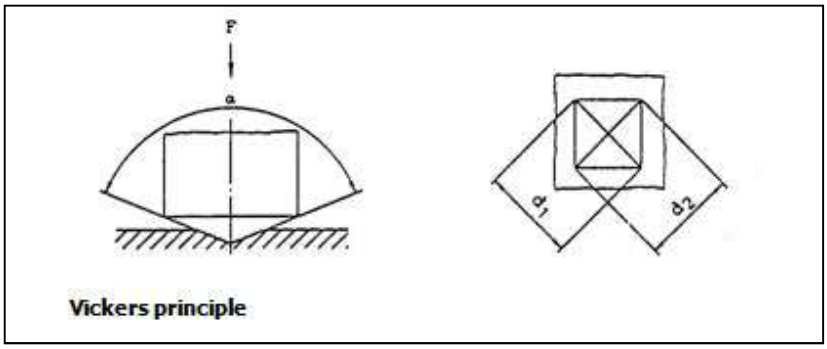

Figure 3.11- Vickers micro hardness indentation

The loads for Micro Vickers or Knoop hardness testing methods are typically very low, ranging from a few grams to 2 kg. The load range for Macro Vickers hardness test procedure can range up to 50kgs.Normally the prepared specimens; using metallographic mounting presses are mounted in a plastic medium to facilitate the preparation and testing. In order to enhance the resolution of measurement, the indentations should be as large as possible. The micro hardness was measured with the help of Vickers micro hardness tester. It was compatible with computer; the indentations formed by indenter can be seen. The load can be takes over the micro hardness tester was upto 100 kg. And the magnification of the indentation was 200 x and 400X. The load selected was 5 gm, because at high load the indenter would be large. The magnification chosen was 400 X, because at that low load indentation was very small.

3.8. Optical Microscope:

It is an instrument used to see objects too small for the naked eye. The science of investigating small objects using such an instrument is called microscopy. Microscopic means invisible to the eye unless aided by a microscope.

Figure 3.12 - Optical microscope

The most common type of microscope and the first invented is the optical microscope (figure 3.14). This is an optical instrument containing one or more lenses producing an enlarged image of a sample placed in the focal plane. Optical microscopes have refractive glass and occasionally of plastic or quartz, to focus light into the eye or another light detector. Mirror-based optical microscopes operate in the same manner. Typical magnification of a light microscope, assuming visible range light, is up to 1500x with a theoretical resolution limit of around 0.2 micrometres or 200 nanometers. Specialized techniques (e.g., scanning confocal microscopy, Vertico SMI) may exceed this magnification but the resolution is diffraction limited. The use of shorter wavelengths of light, such as the ultraviolet, is one way to improve the spatial resolution of the optical microscope, as are devices such as the near-field scanning optical microscope.

4. Result and discussion:

4.1 Coating characterization:

The microstructures of the coating were studied with the help of scanning electron microscope. The microstructures of the coating suggest that the splat of the deposited material does not seem to form a continuous layer but at the cross section, it was observed that the coating was more homogeneous and regular (figure 4.1).

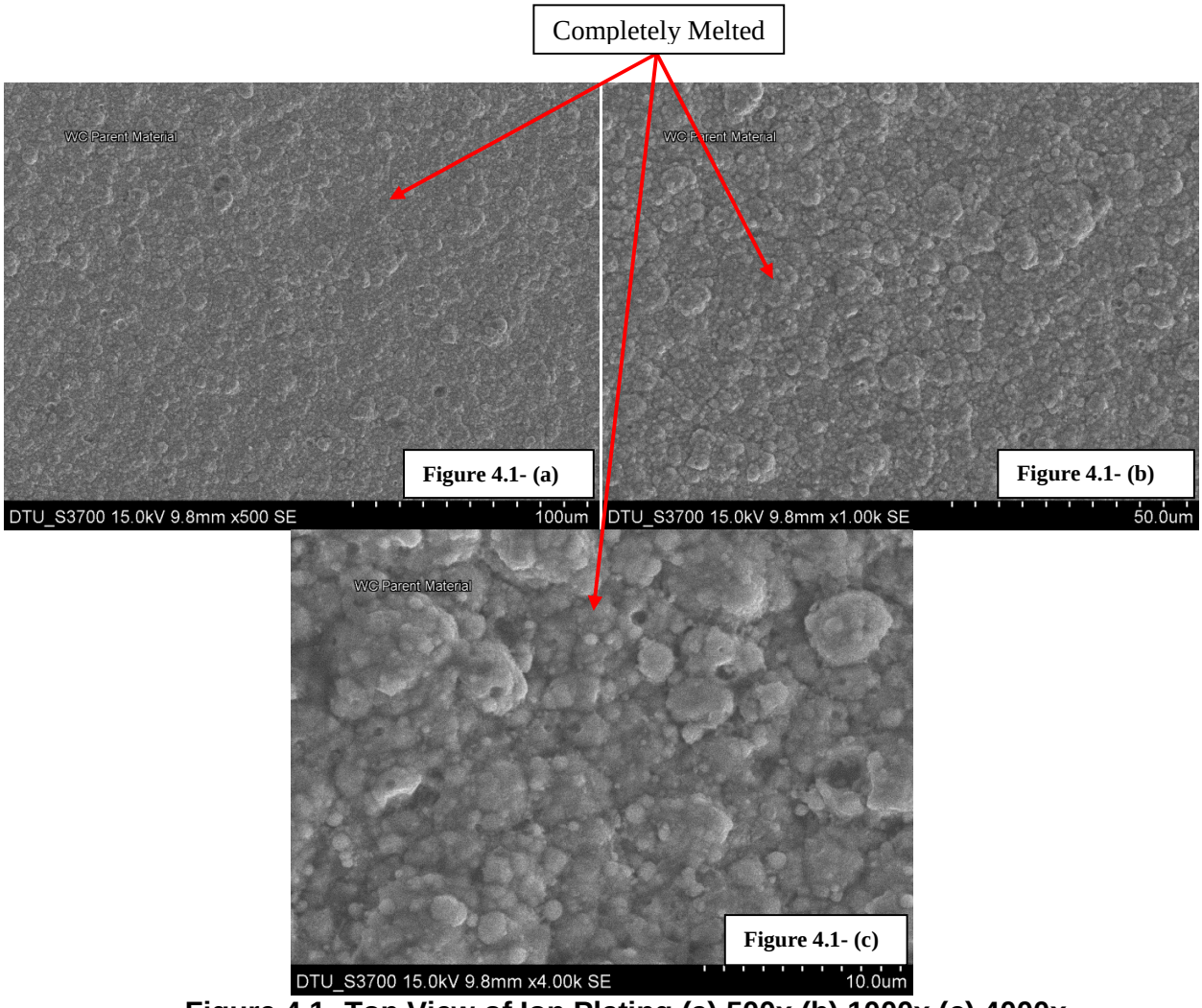

Figure 4.1- Top View of Ion Plating (a) 500x (b) 1000x (c) 4000x

The Ion plating was found in the form of continuous layer with dome shape structure of its particle. The blow holes & porosity were regular (Figure 4.1(c)) having homogeneous structure with complete melted part.

4.2. Wear rate of Ion Plated Disc with Tungsten Carbide, HCS and Mild Steel Pin:

Wear rate of the Ion Plated Disc under the Increasing loading of 40N, 50N, 60N, and 70N with the Increasing sliding speed of 550 RPM, 650 RPM, 750 RPM, and 850 RPM for a constant sliding distance of 2Km were calculated with the weight loss method. By using loads and sliding speed as variables and three different counter bodies (tungsten carbide, HCS, MS), experiment was performed with the pin on disc Tribometer.

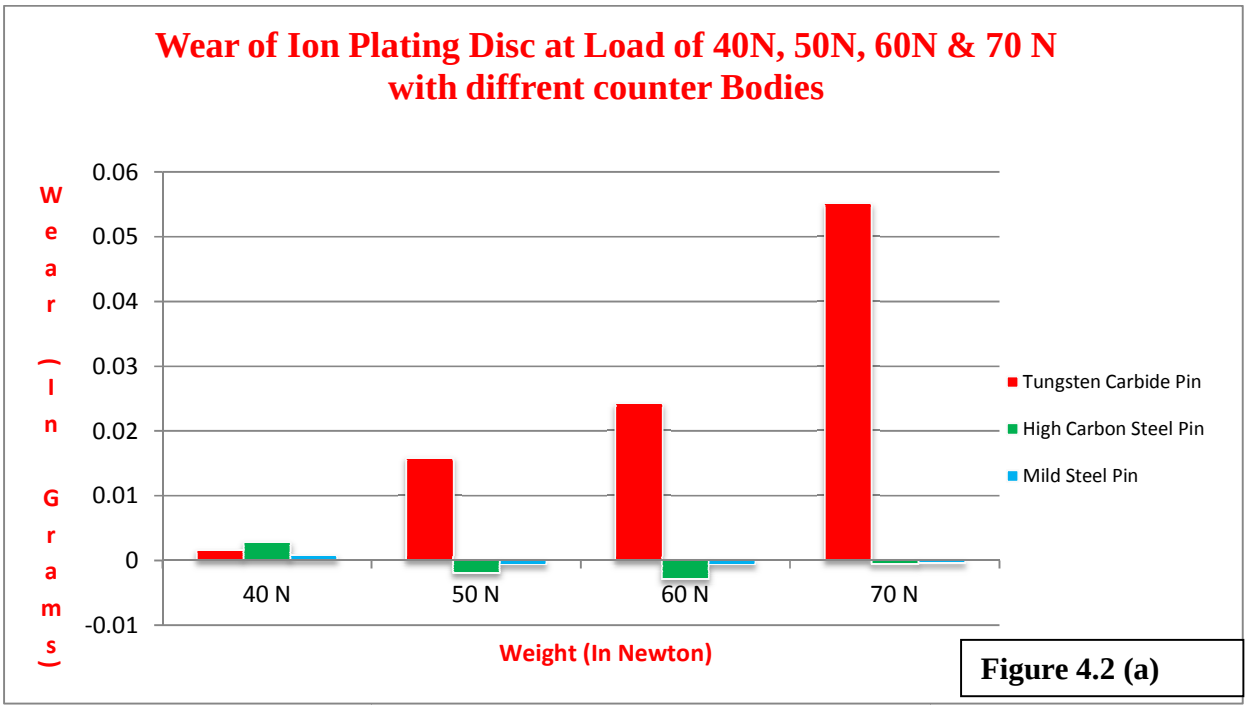

Figure 4.2 (a)

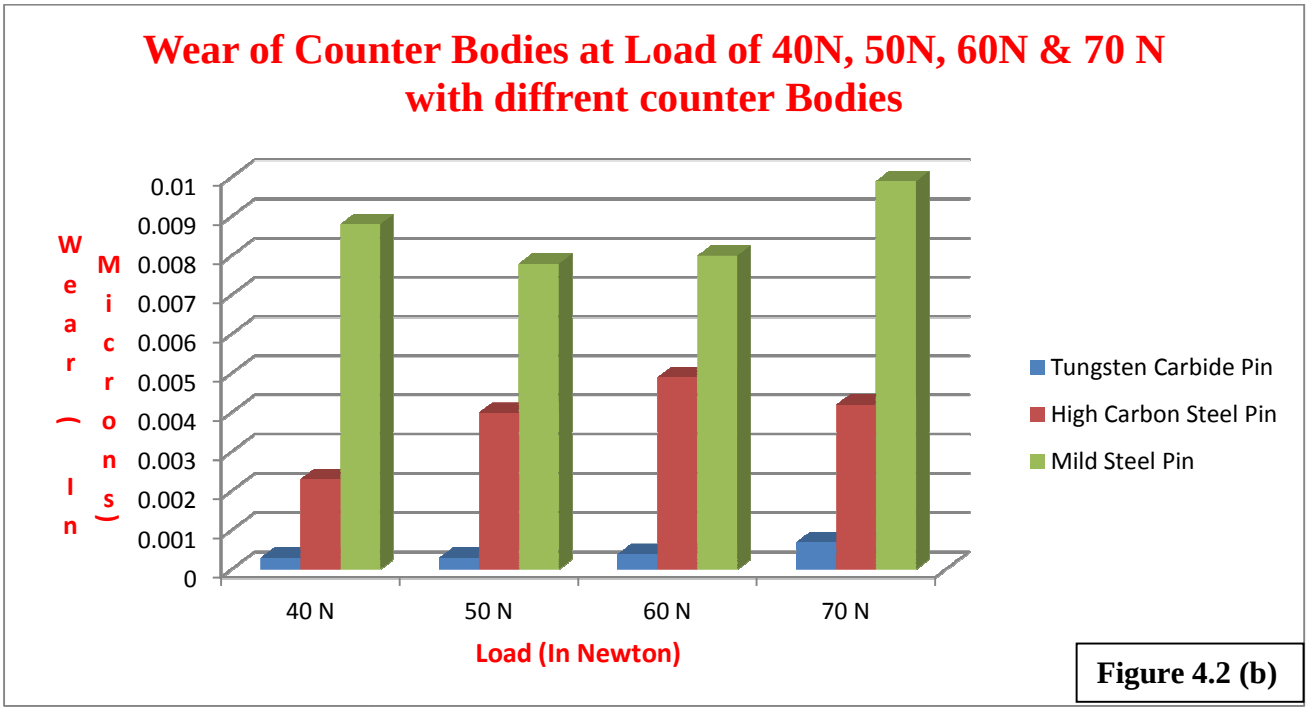

Figure 4.2(a) Shows the variation of the wear rate of the Ion Plated Disc at different loads with different counter bodies.

(b) Shows the variation of the wear rate of the different counter bodies at different loads with Ion Plated Disc.

Figure 4.2 (a&b) shows the variation of the wear rate of the Ion Plated Disc at different load and different counter bodies (Tungsten Carbide, HCS and Mild Steel). The wear rate of the Ion plated disc with the counter body of tungsten carbide at 550 rpm speed, and 40 N load was calculated as 0.0016 g. The wear rate increased to 0.0159 g when the load and speed were increased to 50 N and 650 rpm simultaneously. The wear rate at 60 N loads and 750 rpm further increased to 0.0242 g and again increased to a value of 0.0551g at 70N and 850 rpm. The wear rate of the Ion Plated Disc at 550 rpm speed

with the counter body of HCS, and 40 N loads was 0.0028 g. When the load and speed was further increased to 50 N and 650 rpm; the wear rate decreases to **-0.002g. (Negative Value, Weight Gain of Disc)**. The wear rate further decreased to -0.003 g at the load of 60 N and 750 rpm and -0.0006 g at 70 N and 850 rpm. The wear rate of the coating at 550 rpm , 650 rpm, 750rpm and 850 rpm speed with the counter body of Mild Steel and 40 N, 50 N, 60 N & 70 N loads was calculated as 0.0007 g, -0.0007, -0.0007 and -0.0005 which is almost negligible.

The wear rate of the coating with tungsten carbide pin (WC) was found to be higher than the wear rate of the coating with HCS pin and wear rate of HCS was found to be higher than the wear of the MS pin at the 550rpm & 40N loading condition. The wear rate of the Ion plated disc was found to be increased with the increasing load and sliding speed. But in the case of HCS & MS pin with the increase of loading condition with speed the deposition of pin material on the Ion plated disc started because of which the weight of the ion plated disc increases than the original weight. P.L. Ko et el.[60] in 2002 showed the similar trends of the mass lass rate of the chrome plating with the Al-Ni pin with increase of the speed . Giovanni Borelli et el. in 2006 also reported the decreasing trends of wear rate with the increase of no of revolution [23]. The reason for this decreasing trend in the wear rate is explained by Koji Kato et el. in 2000 as When a triboelement made of soft material such as plastics is rubbed and effectively worn by a harder counterpart, its wear can be reduced by forming a transfer layer of the soft material on the counter surface of harder material. Wear rate of the soft material in sliding against itself must be small in this case [30].

When a tribo-element is made of a material having hardness less than the hardness of the counter body, material in the contact region plastically deforms severely under the combined stresses of compression and shear. Large plastic deformation generally introduces large wear rate since wear surface tends to become rough and protective surface layers are easily destroyed. [30]

W. Maa et al. [51] showed that the wear behavior of different material is different with different counter materials. The wear rate of the coating increased slightly with increased in the sliding speed at low load. But at high load the wear rate increased to a higher value at the increased sliding speed. It case of medium carbon steel pin the material gets eroded fast so the coefficient of friction and the wear rate were found to be more [51, 54]. The wear rate of the coating with tungsten carbide pin was much higher in comparison of HCS and the Mild Steel as the tungsten carbide pin is much harder compared to the Ion Plated Disc, and the wear mechanism was mainly due to micro cutting. The wear because of the HCS and nickel was found to be negligible as Ion Plating is much harder than HCS and Mild Steel.

4.3. Coefficient of friction (CoF) of the Ion Plated Disc with Tungsten Carbide, HCS & Nickel Pin at different loading condition:

The co-efficient of friction (CoF) of chrome coating with En-31, tungsten carbide and nickel pin at different loading condition was analyzed under similar sliding conditions,

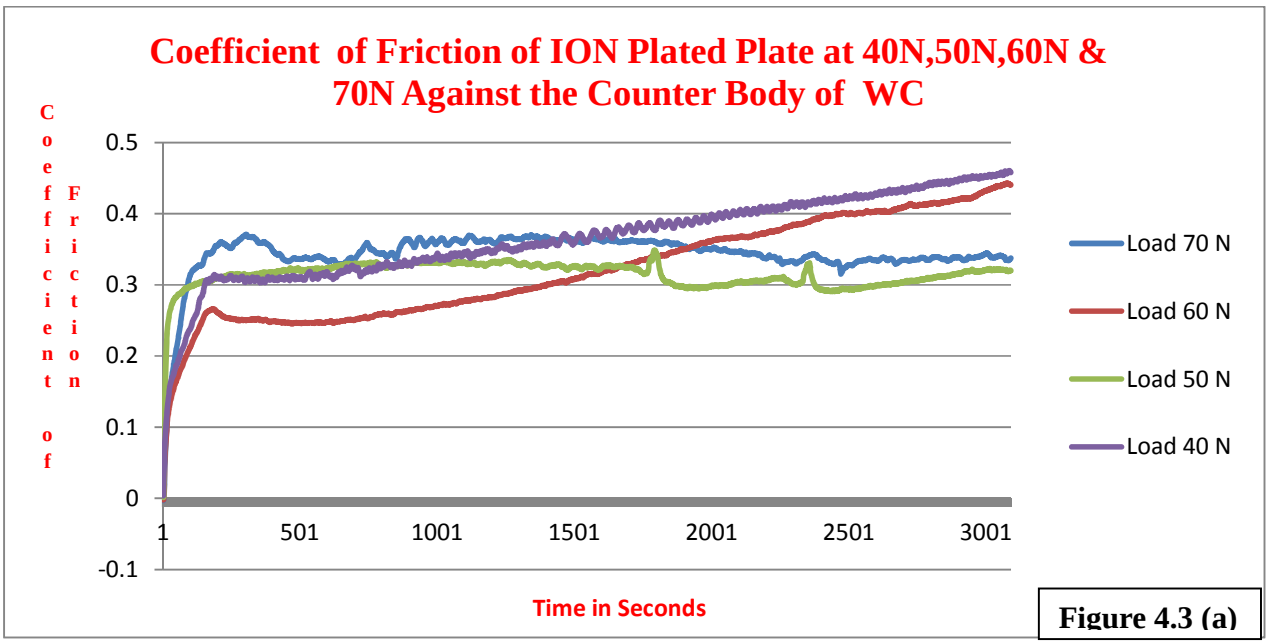

Figure 4.3 (a)

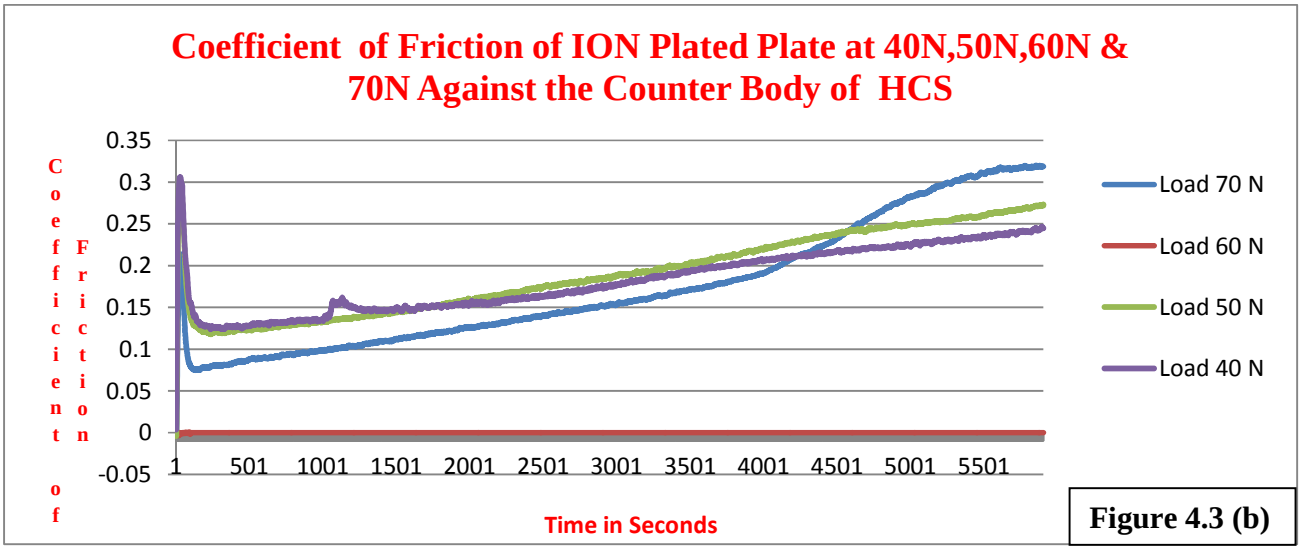

Figure 4.3 (b)

.

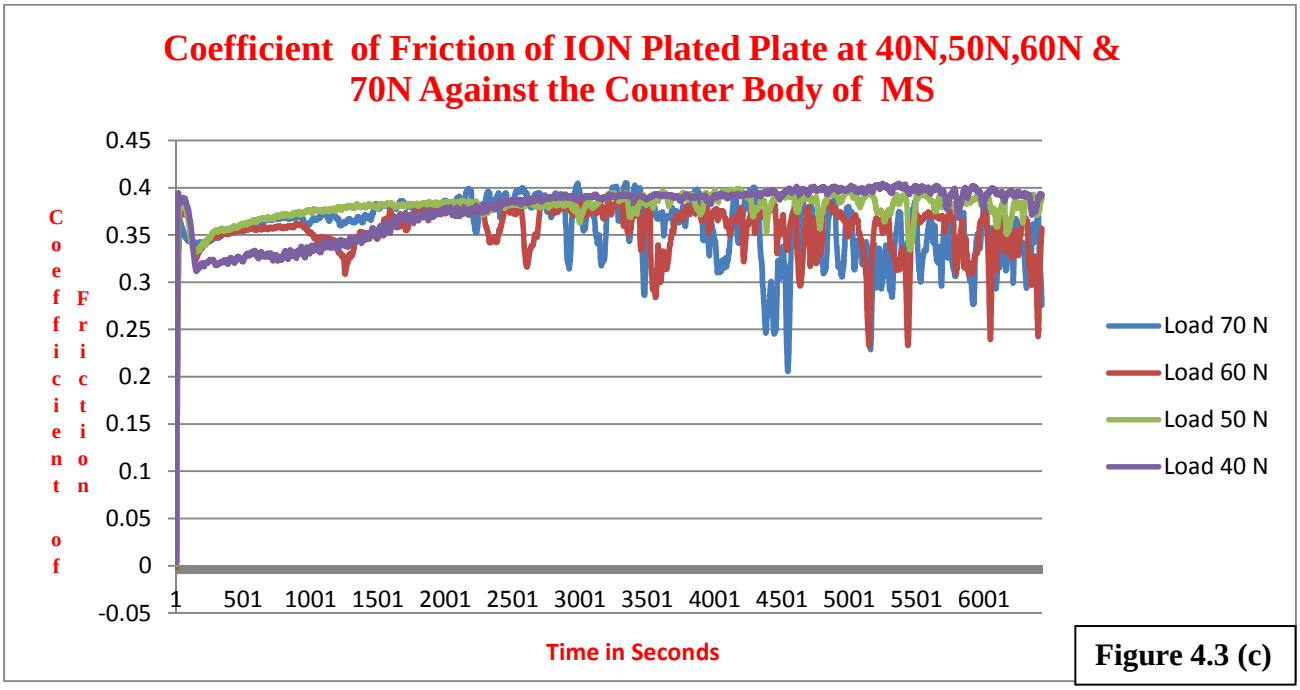

Figure 4.3 (c)

Figure 4.3- (a) Variation of coefficient of friction of Ion Plated Disc with WC pin at various loading and sliding conditions. (b) Variation of coefficient of friction of Ion Plated Disc with HCS pin at various loading and sliding conditions (c) Variation of coefficient of friction of Ion Plated Disc with MS pin at various loading and sliding conditions

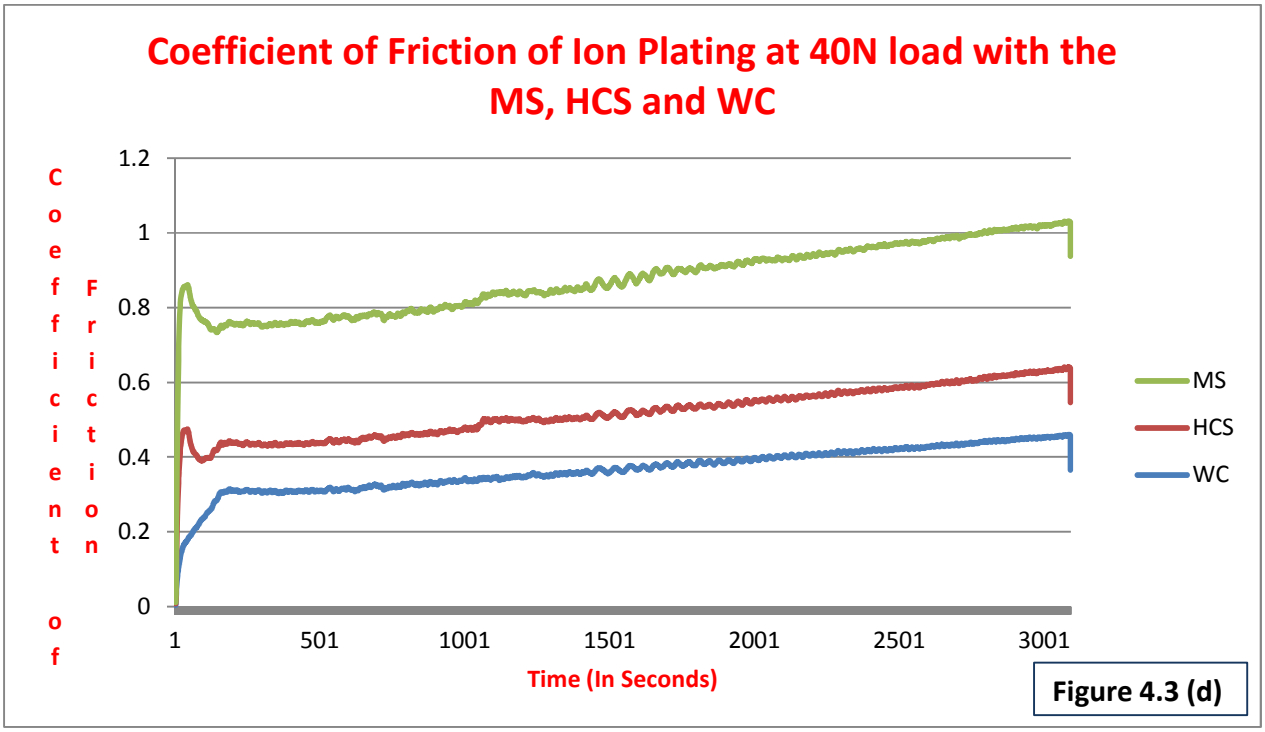

Figure 4.3 (d)

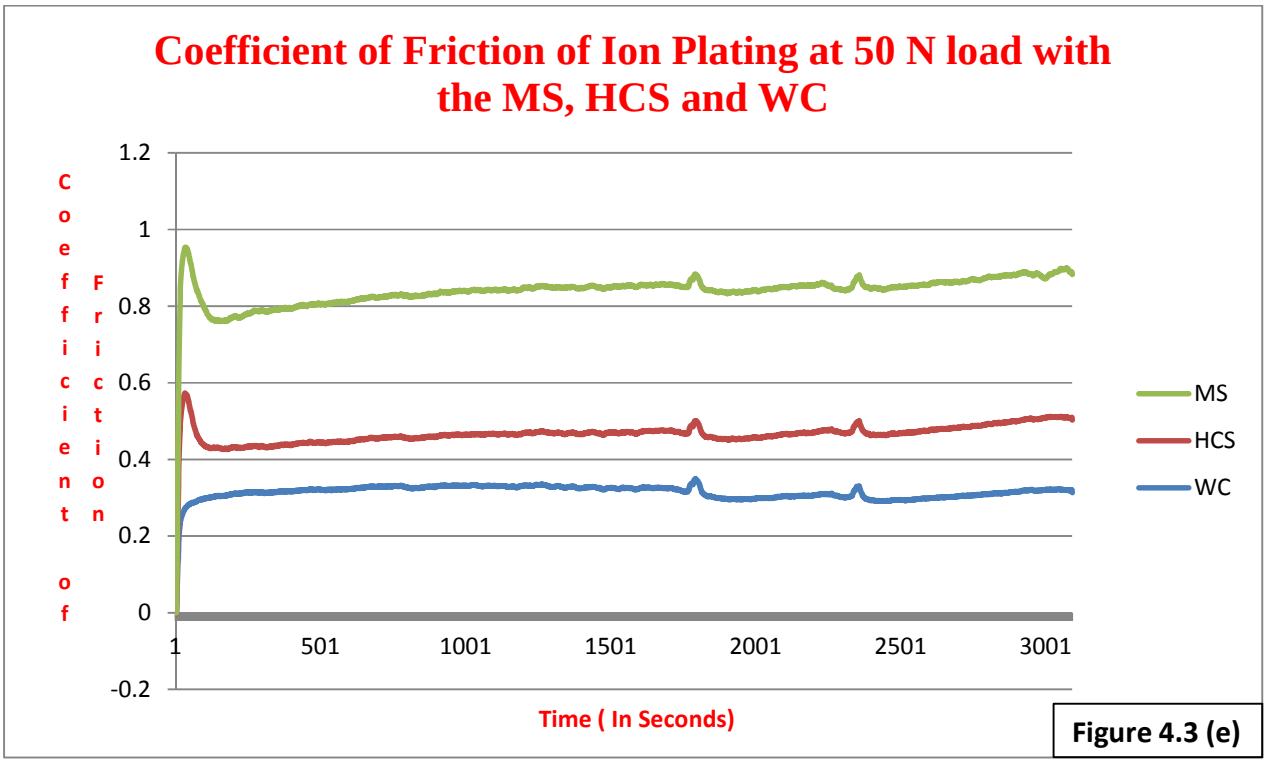

Figure 4.3 (e)

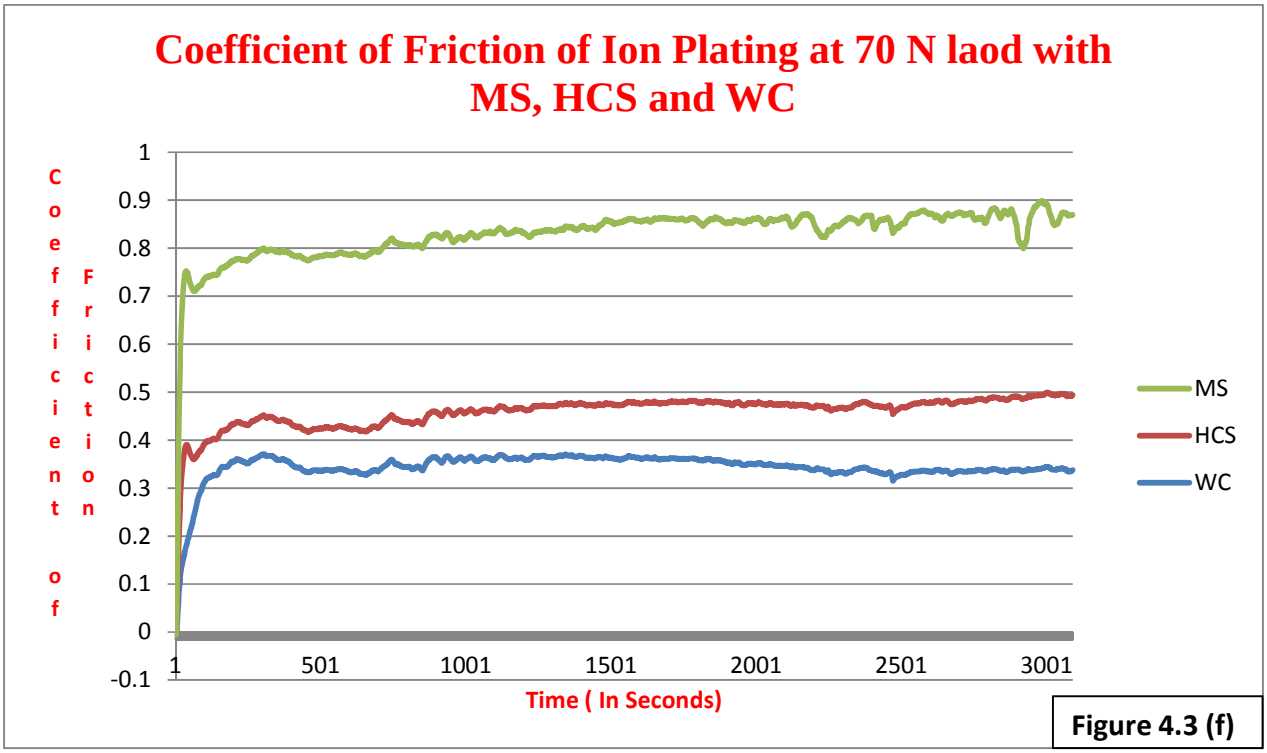

Figure 4.3- (d) Variation of coefficient of friction of Ion Plated Disc with WC, HCS and MS pin at 40 N loading and 550 rpm sliding conditions. (e) Variation of coefficient of friction of Ion Plated Disc with WC, HCS and MS pin at 50 N loading and 650 rpm sliding conditions (f) Variation of coefficient of friction of Ion Plated Disc with WC, HCS and MS pin at 70 N loading and 850 rpm sliding conditions

Figure 4.3 (a, b & c) shows the variation of the co-efficient of friction of Ion plating at different loading and sliding condition with WC, HCS and Mild steel pin.The coefficient of friction of the Ion plating with the counter body of WC at 40.0 N load and 550 rpm was found to be 0.3654. The coefficient of friction was found decrease to 0.3140 at a load of 50.0 N at the same 550 rpm speed. When the load was increased to 60 N at the 650 rpm sliding speed the co-efficient of friction found to be increased to 0.3202 and to 0.3433 at 70 N & 850rpm. The co-efficient of friction of the Ion plating with HCS at 550 rpm speed and 40 N load was 0.1820 With the increased of load to 50.0 N at the 650 rpm sliding speed it again decreased to 0.1810. It found to be decreased at 1739, when

the load was increased to 70 N at the 850 rpm sliding speed. The co-efficient of friction with MS pin at 550 rpm speed and 40.0 N load was 0.3760. It increased to 0.3795, when the load was increased to 50.0, at the 650 rpm sliding speed. The co-efficient of friction found to be decreased to 0.3558 at 60 N load and 650 rpm sliding speed. and .3550 at 70 N & 850 rpm.

Figure 4.3 (d, e & f) showed the coefficient of friction of the Ion Plated Disc with the WC, HCS and MS at different load. Figure 4.3 (d, e, and f) shows that the CoF of MS with Ion Plated Disc is higher than HCS, HCS have the higher CoF than WC at the load of 40N, 50N and 70 N at sliding speed of 550, 650 & 850 respectively. The coefficient of friction was decreased with increased loading conditions. It was decreased may be due to reason that at increased load, the wear rate was more, that's why the direct rubbing was less. And it showed less coefficient of friction. The co efficient of friction is low when the load is high and sliding speed is high [12, 53]. The Binshi Xu et al. [9] found that the coefficient of friction of aluminum alloy decreases with an increase in load.

4.4 Wear mechanism of Ion Plated Disc with WC, HCS and MS Pin:

When the tungsten carbide pin slides over the Ion Plated Disc at 550 rpm speed and 40 N load then abrasion of the coating was more and the wear debris was in the form of microchips (figure 4.4 c)

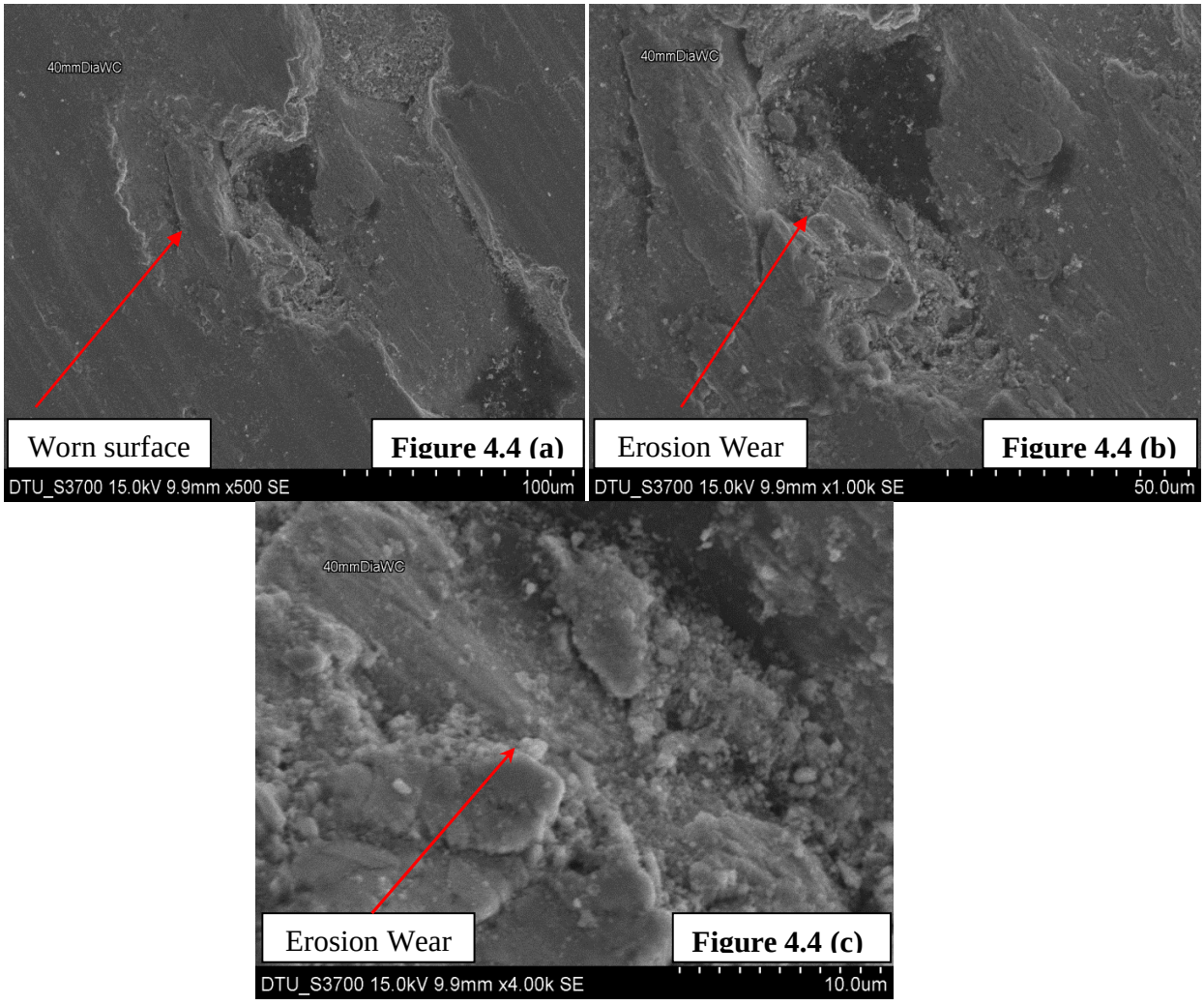

Figure 4.4 - Worn surfaces Ion Plated Disc with WC at 550 rpm speed & 40N Load (a) 500 X (b) 1000 X (c) 4000 X

These microchips were suddenly removed over the track due to high velocity. At 50 N load and 650 rpm speed deformation was found to be more, due to high pressure exerted by the pin. The worn debris also got deposited over the wear track.

When the wear load was further increased to 60 N and speed at 750 rpm, there was more deformation of the coating surfaces. With HCS & MS the pin material got deformed and the diffusion observed was more, whereas in case of tungsten carbide pin the pin did not get deformed (Figure 4.7 a, b ,c & d). At this speed with the tungsten carbide pin the wear behavior was not only due to abrasion but also due to deformation, the coating surfaces get deformed and adhered over the surface

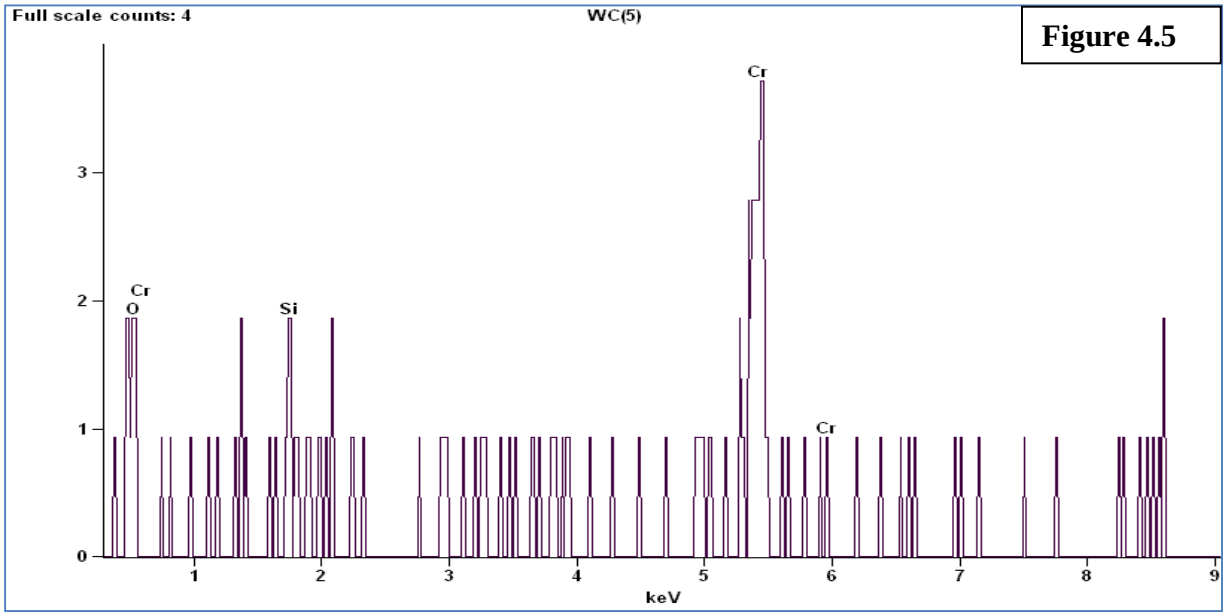

Figure: 4.5 EDS Graph of Wear Track of Ion Plated Disc with counter Body of WC

Element Line	Net Counts	Int. Cps/nA	Weight %	Weight % Error	Atom %	Atom % Error	Formula	Standard Name
O K	10	0.000	13.94	+/- 2.79	33.54	+/- 6.71	O	
Si K	4	0.000	4.38	+/- 3.29	6.00	+/- 4.50	Si	
Si L	0	0.000	---	---	---	---		
Cr K	30	0.000	81.68	+/-16.34	60.45	+/-12.09	Cr	
Cr L	0	0.000	---	---	---	---		
Total			100.00		100.00			

Table 4.1 EDs of the Wear Track of Ion plated Disc with the counter body of WC

This is also supported by the EDS graphs & table of the wear track at 40N & 550rpm that there is no deposition of the tungsten on the wear track.

At a load of 40 N load and 550 rpm with the HCS pin deformations were less and Erosion was the major wear mechanism (Figure 4.6 a, b, c). If the load was increased to 50 N at the 650 rpm speed, the deformation of the HCS pin was more. At 60 N loads and 750 rpm speed, the HCS & MS pin got deformed and deposited over the coating surface forming a thin layer hence the surface was found smooth. Slow speed caused more plastic deformation of the coating material and the abrasion of the coating was less.

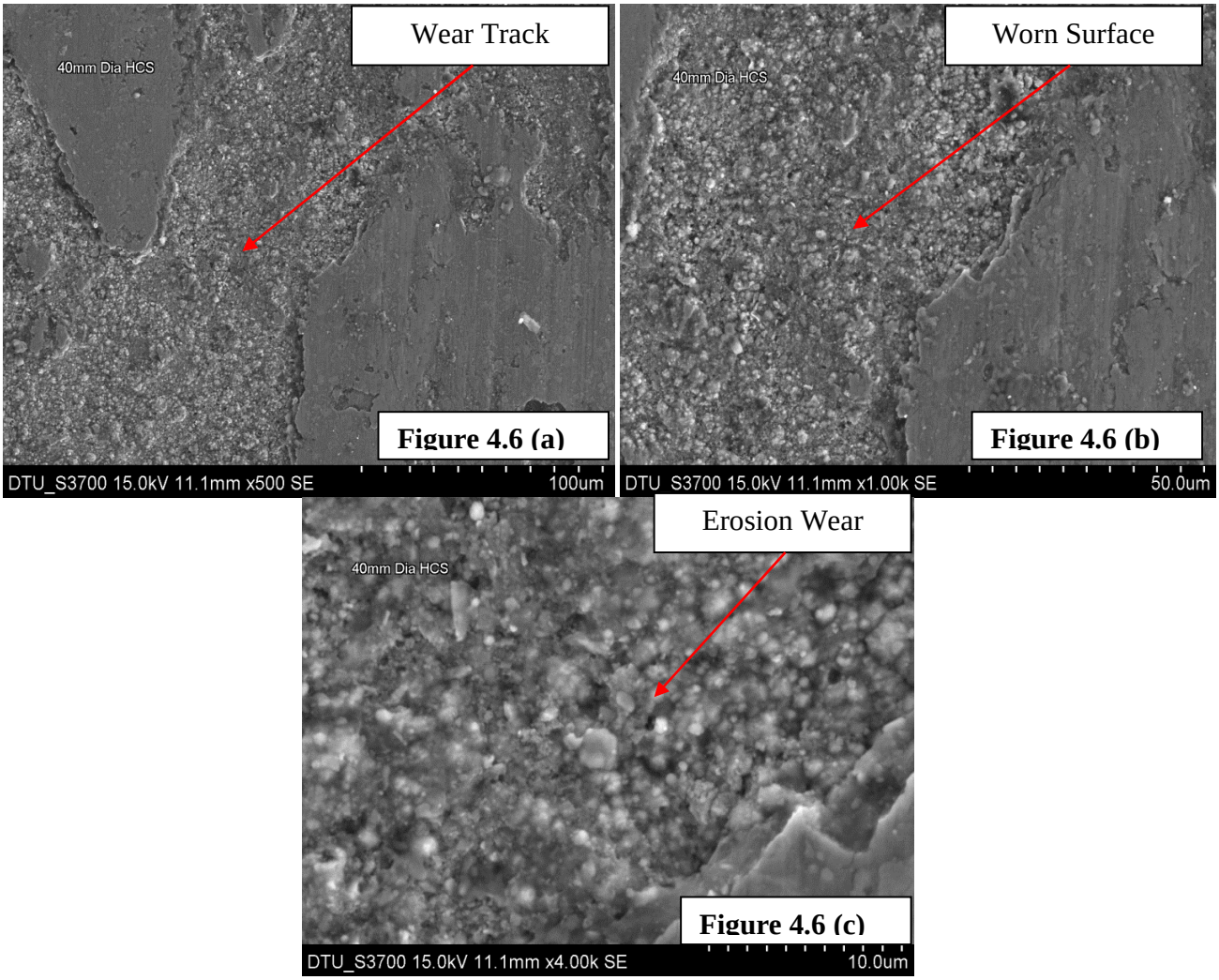

Figure 4.6 - Worn surfaces of Ion Plated Disc with HCS pin at 750 rpm speed & 60 N Load (a) 500 X (b) 1000 X (c) 4000 X

The wear behavior at 550rpm speed and a load of 40 N with MS was also studied and it was found that at this load, the shear of the pin material was more (Figure 4.8 a, b, c & d) and the coating was less deformed due to softness of the pin material in respect to Ion Plating. When the load was further increased to 50 N & 650 rpm over the pin then the shear observed was more and the plastic deformation of the coating was high. At higher load of 60 N & 750 rpm the wear rate of the coating increased, the micro cutting of the coating was high and the deformation of the coating was less.

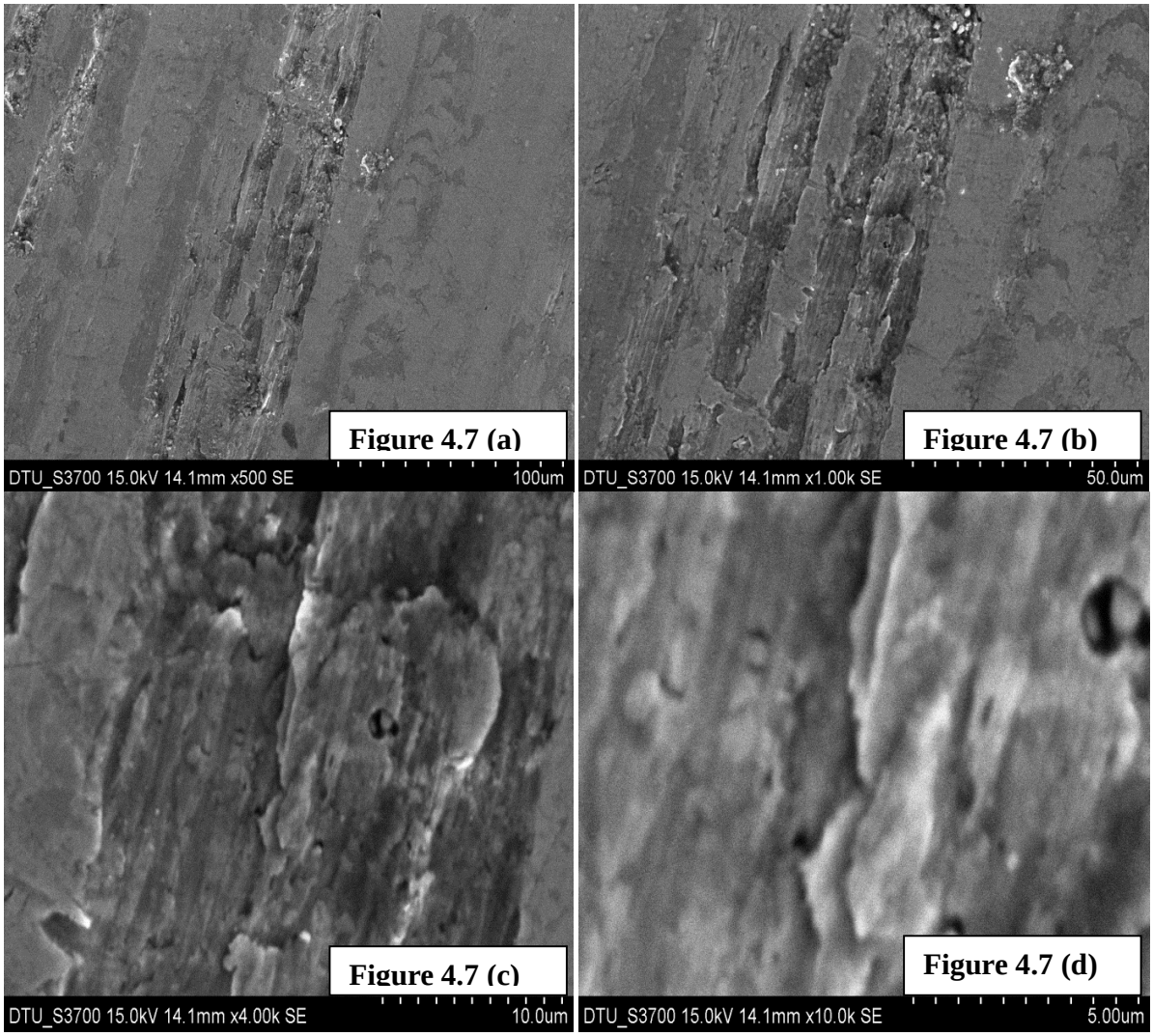

Figure 4.7 Worn surfaces of HCS pin against the Ion Plated Disc (a) 500X (b) 1000X (c) 4000X (d) 10000X

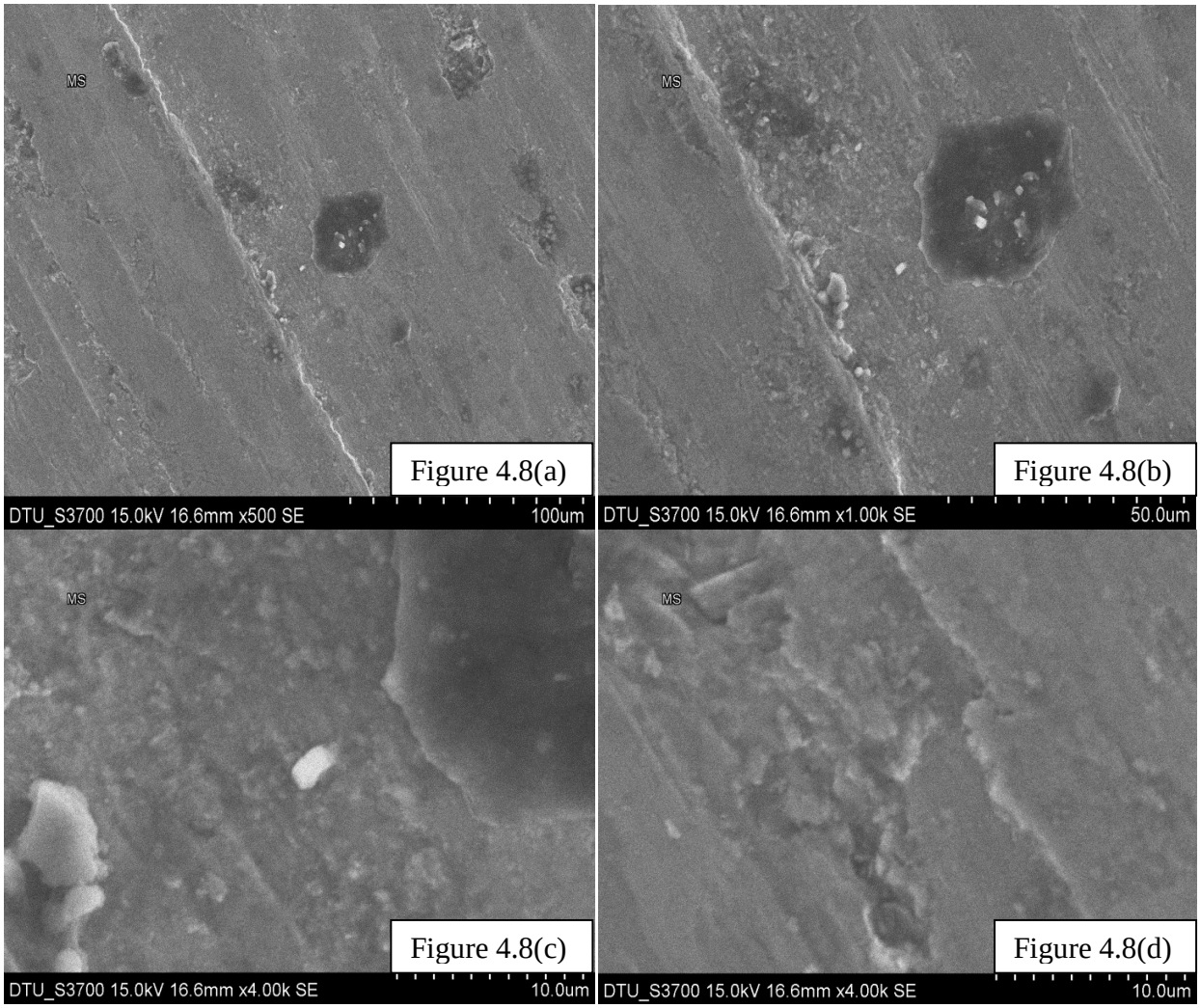

Figure 4.8 Worn surfaces of MS pin against the Ion Plated Disc (a) 500X (b) 1000X (c) 4000X (d) 10000X

At 550 rpm speed and 40 N load with the tungsten carbide pin the deformation was high as compared to deformation in case of HCS & MS at same loading condition. When the load was increased to 50 N at the 650 rpm speed with the tungsten carbide pin the deformation as well as micro cuttings were also increased. At 60 N load and 750 rpm speed deformation was much higher along with the micro cutting and abrasion

At 550 rpm speed and 40 n load with HCS pin the deformation as well as micro cutting was less, along with less deformation of the wear track. At the 650 speed and load of 50

N the deformation of the Pin was more pronounced together with the shear of the coating, but less than that at tungsten carbide.

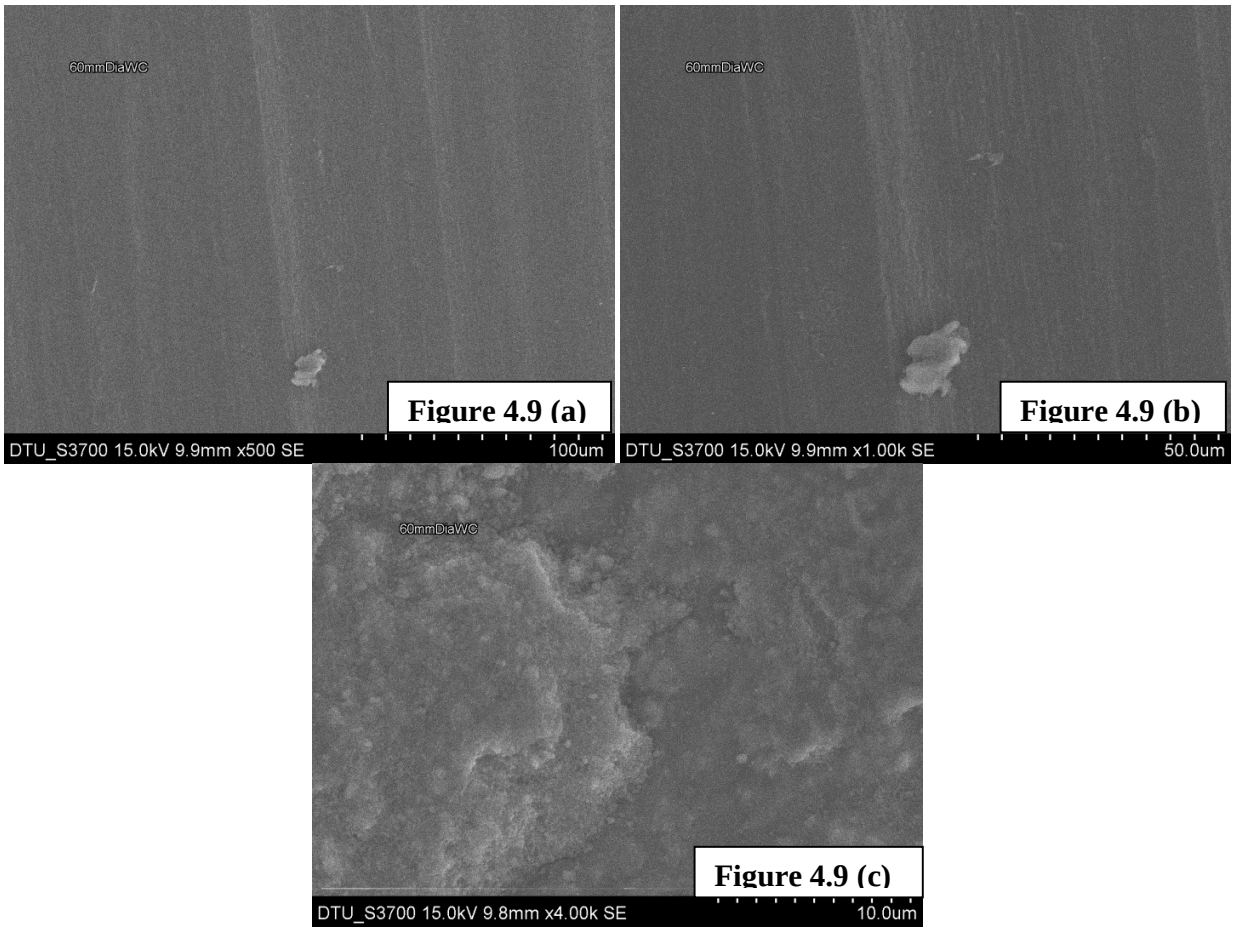

Figure 4.9- Worn surfaces of Ion Plated Disc with tungsten carbide at 550 rpm speed and 40N load (a) 500 X (b) 1000 X (c) 4000 X

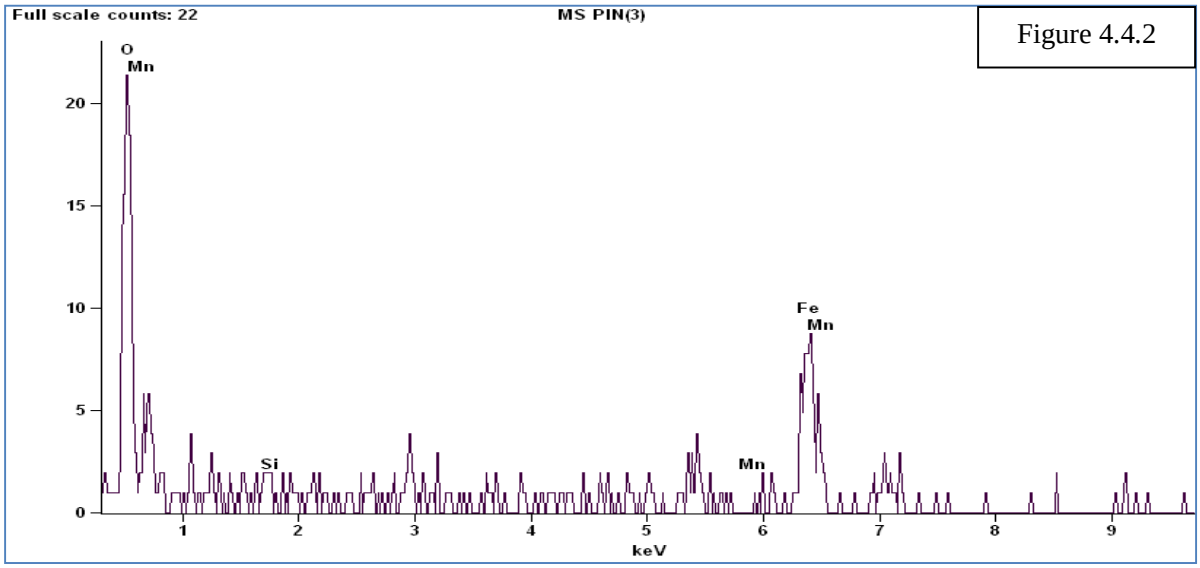

Figure 4.4.2

Figure: 4.10 EDS Graph of Wear Track of Ion Plated Disc with counter Body of MS

Element Line	*Net Counts*	*Int. Cps/nA*	*Weight %*	*Weight % Error*	*Atom %*	*Atom % Error*	*Formula*	*Standard Name*
C K	3	0.000	0.72	+/- 1.67	1.96	+/- 4.58	C	
O K	149	0.000	26.51	+/- 1.78	54.47	+/- 3.66	O	
Si K	10	0.000	1.25	+/- 0.50	1.46	+/- 0.58	Si	
Si L	0	0.000	---	---	---	---		
Mn K	0	0.000	0.00	---	0.00	+/- 0.00	Mn	
Mn L	6	0.000	---	---	---	---		
Fe K	124	0.000	71.53	+/- 9.81	42.10	+/- 5.77	Fe	
Fe L	49	0.000	---	---	---	---		
Total			100.00		100.00			

Table 4.2 EDS of the Wear Track of Ion plated Disc with the counter body of MS

The presence of Mn & Si Counts on the wear track of Ion Plated Disc (Figure 4.5, 4.10, Table 4.1 & Table 4.2) with MS & HCS shows the deposition & deformation of the MS & HCS on the wear track. The table also supports the negative wear of the Ion plated Disc against the counter bodies of HCS & MS. Because of the deposition of the MS & HCS on the Ion Plated Disc the weight of the Ion Plated Disc Increased from its original value.

5. Conclusions:

1. The wear rate of the coatings can be found with the help of pin on disc test under dry sliding conditions.

2. The design of experiment showed that the variable chosen that was load (40, 50, 60 & 70 N) with the Ion Plated Disc and increasing sliding speed (550,650,750,850 RPM) and their interaction was significant.

3. The wear rate was depended on the load and sliding speed. With increase in load the wear rate was found to be increased. The wear rate was also found depend on the pin material, the wear rate in case of Tungsten carbide pin was higher than that of high carbon steel pin & MS. The wear rate of coating primarily depends on sliding speed. With the increase of Sliding speed the wear rate increases at high rate.

4. The coefficient of friction was found low at high load and high sliding speed condition. The coefficient of friction of Ion Plating with WC pin at 40 N & 550 rpm was found to be 0.3654. It was found decreased to 0.3140 at a load of 50 N and 650 rpm. The coefficient of friction of the Ion plating at the 40 N loads & 550 rpm with HCS was found to be 0.1820. It was found increased to 0.1908 at a load of 50 N and the sliding speed 650rpm. The coefficient of friction of Ion Plating with MS at 40N & 550 rpm was found 0.3760. When the load was increased to 50 N & 650 rpm the co-efficient of friction was increased to 0.3795

5. The SEM micrographs showed that the wear mechanism of the coating was accompanied by abrasion, micro cutting and adhesion.

6. The rise of temperature during the wear test was very low due to high heat conduction capacity of capacity of coatings.

7. The coatings can be used for piston rings, and can be used for cylinder liner or for light weight and high strength application such as bonnet and bumper of cars.

6. Future scope of this study:

The coatings can be used for the different type applications such marine applications, scratch resistance, fretting resistance and corrosion resistance applications etc. For its applications many tests on coating has to be performed. The coating can be subjected to 3-point bent test to check the bending strength. The optimization of the coatings techniques such as air plasma arc spray coatings & Ion plating can be done by using the process parameter of the coating machine. We can also perform coating characterization and study the effect of different type of constituent in the coating powder such as effect of the Molybdenum on the coating characteristic. The effects of the particle size on the coatings characteristics can also be studied using different type of analytical techniques. The Similarly, a cladding of carbon fiber can be applied on the coating so that it becomes stiffer as compared to the coating alone. It is expected that the cladding of carbon fiber would increase the tensile strength and stiffness of the coating. The tensile strength of cladded coating can be test over the universal testing machine. The application of carbon cladding also increases the fatigue strength of the coating. Carbon fiber cladded coating can be used for less weight and high strength applications such as car bonnet, bumper etc. Likewise, the coating can be subjected to fretting wear test to check the fatigue strength of the coating. The effects of the temperature on the wear rate can also be determined. The coatings can be further subjected to scratch test so that it can be used as scratch resistance coating on vehicles bonnet and bumper. Erosion test of the coating can be performed to find erosion properties, for potential marine applications.

LIST OF TABLES

Sr. Number	Title	Page No.
Table 3.1	Composition of the test sample prepared	53
Table 3.2	Variables for wear test	61
Table 3.3	Design of experiment table for wear test	61
Table 4.1	EDs of the Wear Track of Ion plated Disc with the counter body of WC	83
Table 4.2	EDS of the Wear Track of Ion plated Disc with the counter body of MS	88

References

01 L. Fedrizzi, S. Rossi, F. Bellei, F. Deflorian, Wear–corrosion mechanism of hard chromium coatings, Wear 253 (2002) 1173–1181.

02 W.H Dennis, Metallurgy of non ferrous metals, London, Sir Isaac pitman & sons ltd, 2002**.**

03 A.A. Boudi, M.S.J. Hashmib, B.S. Yilbas "HVOF coating of Inconel 625 onto stainless and carbon steel surfaces: corrosion and bond testing" Journal of Materials Processing Technology 155–156 (2004) 2051–2055.

04 Junius David Edwards, Aluminum and its production, assistant director of research, aluminum company of America, 1999.

05 J. Voyer, B.R. Marple, Sliding wear behavior of high velocity oxy-fuel and high power plasma spray-processed tungsten carbide-based cermets coatings, Wear 225–229 (1999) 135–145.

06 Z. N. Farhat, Y. Ding, A. T. Alpas and D. O. Northwood, The Processing and Testing of New and Advanced Materials for Wear Resistant Surface Coatings, Journal of Materials Processing Technology 63 (1997) 859-864.

07 Y. Xie, H.M. Hawthorne, Wear mechanism of plasma-sprayed alumina coating in sliding contacts with harder asperities, Wear 225–229 (1999) 90–103.

08 B. Torres, M.A. Garrido, A. Rico, P. Rodrigo, M. Campo, J. Rams, Wear behavior of thermal spray Al/Sic coatings, Wear 268 (2010) 828–836.

09 Binshi Xua, Zixin Zhua, Shining Maa, and Wei Zhang, Weimin Liu, Sliding wear behavior of Fe–Al and Fe–Al/WC coatings prepared by high velocity arc spraying, Wear 257 (2004) 1089–1095.

10 J. Voyer, B.R. Marple, Sliding wear behavior of high velocity oxy-fuel and high power plasma spray-processed tungsten carbide-based cermets coatings, National Research Council Canada.

11 E. Fernandez, M. Cadenas, R. Gonzalez, C. Novas, R. Fernandez, J. de Damborenea, Wear behaviour of laser clad NiCrBSi coating, Wear 259 (2005) 870–875.

12 R. Gonzalez, M. Cadenas, R. Fernandez, J.L. Cortizo, E. Rodriguez, Wear behavior of flame sprayed NiCrBSi coating remelted by flame or by laser, Wear 262 (2007) 301–307.

13 Y. Iwai a, T. Honda, H. Yamadaa, T. Matsubara, M. Larsson, S. Hogmarkd, Evaluation of wear resistance of thin hard coatings by a new solid particle impact test, Wear 251 (2001) 861–867.

14 K.S. Tan, J.A. Wharton, R.J.K. Wood, Solid particle erosion–corrosion behaviour of a novel HVOF nickel aluminum bronze coating for marine applications—correlation between mass loss and electrochemical measurements, Wear 258 (2005) 629–640.

15 Gedzevicius, A.V. Valiulis, Analysis of wire arc spraying process variables on coatings properties, Journal of Materials Processing Technology 175 (2006) 206–211.

16 V.E. Buchanan, D.G. McCartney, P.H. Shipway, A comparison of the abrasive wear behaviour of iron-chromium based hard faced coatings deposited by SMAW and electric arc spraying, Wear 264 (2008) 542–549.

17 Ozkan Sarikaya, Selahaddin Anik, Erdal Celik, S. Cem Okumus, Salim Aslanlar, Wear behaviour of plasma-sprayed AlSi/B_4C composite coatings, Department of Mechanical Engineering, Esentepe Campus, Sakarya, Turkey, 27 September 2006.

18 M. Grujicic, C.L. Zhao, W.S. De Rosset, D. Helfritch, Adiabatic shear instability based mechanism for particles/substrate bonding in the cold-gas dynamic-spray process, Department of Mechanical Engineering, Clemson University, Clemson, USA, 7 June 2004.

19 C. Zhang, X.P. Guo, G. Zhang a, H.L. Liao, C. Coddet, Effect of standoff distance on coating deposition characteristics in cold spraying, Jiao tong University, Materials and Design 29 (2008) 297–304.

20 R. L. Deuis, C. Subramanian & J. M. Yellupb, Dry sliding wear of aluminum composites-a review, Composites Science and Technology 57 (1997) 415-435.

21 Alexey V. Byeli, Marat A. Belotserkovskii, Vladimir A. Kukarekob, Microstructure and wear resistance of thermal sprayed steel coatings ion beam implanted with nitrogen, Joint Institute of Mechanical Engineering, Belarus.

22 V. Raj, M. Mubarak Ali, Formation of ceramic alumina nanocomposite coatings on aluminum for enhanced corrosion resistance, Department of Chemistry, Periyar University, Salem 636 011, India.

23 Giovanni Borelli, Valeria Cannillo, Luca Lusvarghi, Tiziano Manfredini, Wear behavior of thermally sprayed ceramic oxide coatings, Wear 261 (2006) 1298–1315.

24 H.McI Clark, H.M. Hawthorne, Y. Xie, Wear rates and specific energies of some ceramic, cermets and metallic coatings determined in the Coriolis erosion tester, Wear 233–235 (1999) 319–327.

25 Curran, J.A Clyne, The thermal conductivity of plasma electrolytic oxide coatings on aluminum and magnesium, Surf. Coating Technology 1999, 177–183.

26 H. Duan, C. Yan, F. Wang, Effect of electrolyte additives on performance of plasma electrolytic oxidation films formed on magnesium alloys, Electrochemical Acta. 52, 3785–3793.

27 Zhenbing Caia, Minhao Zhua, Huoming Shenb, Zhongrong Zhoua, Xuesong Jin, Torsion fretting wear behavior of 7075 aluminum alloy in various relative humidity environments, Southwest Jiao tong University, Chengdu 610031, China.

28 Yi Maozhonga, Huang Baiyun, He Jiawenb, Erosion wears behavior and model of abradable seal coating, Wear 252 (2002) 9–15.

29 Wear and Lubrication, Glossary of terms and definition in the field of Friction, (Tribology), Research Group on Wear of Engineering Materials, OECD, Paris, 1969.

30 Koji Kato, Wear in relation to friction — a review, Wear 241 (2000) 151–157.

31 A.P. Sannino, H.J. Rack, Dry sliding wear of discontinuously reinforced aluminum composites review and discussion, Materials Science and Engineering Program, Department of Mechanical Engineering, Clemson University, Clemson, SC 29634-0921 USA, Wear 189 (1995) 1-19.

32 M. Singh, D.P. Mondal, O.P. Modi, A.K. Jha, Two-body abrasive wear behaviour of aluminum alloy–sillimanite particle reinforced composite, Wear 253 (2002) 357–368.

33 Nizamettin Kahramana, Behcet Gulenc¸, Abrasive wear behavior of powder flame sprayed coatings on steel Substrates, Materials and Design 23 (2002) 721–725.

34 Satoh T, Koreeda N, Hayashi T, Nagai M., Fretting fatigue properties of turbine blade/disk joints, Technical Research and Development Institute, Japan Defense Agency Technical Report No. 6687, 1999.

35 Torres Y, Rodriguez S, Mateo A, Anglada M, and Llanes L., Fatigue behavior of powder metallurgy high-speed steels: fatigue limits prediction using a crack growth threshold-based approach, Mater Sci. Engg. a Structure Mater 2004;387–389:501–4.

36 J. Takeda, M. Niinomi, T. Akahori, Gunawarman, Effect of microstructure on fretting fatigue and sliding wear of highly workable titanium alloy (Ti–4.5Al–3V–2Mo–2Fe), Toyohashi, Japan 19 December 2003.

37 T. Kachele, Recent research results on predicting and preventing silt erosion, Proceedings of the First International Conference on Silting Problems in Hydropower Plants, October 1999, India, 1999.

38 Yucong Wang, Simon, Tung, Scuffing and wear behavior of aluminum piston skirt coatings against aluminum cylinder bore, Wear 225–229 (1999) 1100–1108.

39 Rahul Premachandran Nair, Drew Griffin, Nicholas X. Randall, The use of the pin-on-disk Tribology test method to study three unique industrial applications, Wear 267 (2009) 823–827.

40 Garcia-Prieto, M.D. Faulkner, J.R. Alcock, The influence of specimen misalignment on wear in conforming pin on disk tests, Wear 257 (2004) 157–166.

41 D.K. Dwivedi, T.S. Arjun, P. Thakur, H. Vaidya, K. Singh, Sliding wear and friction behavior of Al–18% Si–0.5% Mg alloy, Journal of Materials Processing Technology 152 (2004) 323–328.

42 Ozkan Sarikaya, Selahaddin Anik, Erdal Celik, and S. Cem Okumus, Salim Aslanlar, Wear behavior of plasma-sprayed AlSi/B_4C composite coatings, Materials and Design 28 (2007) 2177–2183.

43 Alpas, A. T. and Zhang, J., Effect of Sic particulate reinforcement on the dry sliding wear of aluminum silicon alloys (A356), Wear, 1992, 155, 83-104.

44 Alpas, A. T. and Zhang, J., Wear rate transitions in cast aluminum-silicon alloys reinforced with Sic particles, Scripta Metall., 1992, 26, 505-509.

45 Singh, L. and Alpas, A. T., Elevated temperature wear of A16061 and A16061-20%Al, Scripta Metall. Mate, 1995, 32, 1099-1105.

46 Zhang, J. and Alpas, A. T., Delamination wears in ductile materials containing second phase particles, Materials and Design 28 (2007) 2177–2183.

47 Suzuki, High-resolution scanning electron microscopy of immunogold-labelled cells by the use of thin plasma coating of osmium, Journal of Microscopy 208 (3): 153–157.

48 Jeffree, C. E.; Read, Ambient- and Low-temperature scanning electron microscopy, Electron Microscopy of Plant Cells, London: Academic Press. pp. 313–413. ISBN 0123188806.

49 Karnovsky, A formaldehyde-glutaraldehyde fixative of high osmolality for use in electron microscopy, Journal of Cell Biology 27: 137A.

50 Kiernan, Formaldehyde, formalin, Paraformaldehyde and glutaraldehyde: What they are and what they do, Microscopy Today 2000 (1): 8–12.

51 W. Maa, J. Lua, B. Wanga, Sliding friction and wear of Cu–graphite against 2024, Wear 266 (2009) 1072–1081.

52 Subramanian, On mechanical mixing during dry sliding of aluminium-12.3 wt% silicon alloy against copper. Wear, 1993, 161, 53-60.

53 Edrisy, T. Perry, Y.T. Chengb, A.T. Alpas, Wear of thermal spray deposited low carbon steel coatings on aluminum alloys, Wear 251 (2001) 1023–1033.

54 Masaaki Yamane, Tadeusz A. Stolarskia, Shogo Tobeb, Influence of counter material on friction and wear performance of PTFE–metal binary coatings, accepted 23 July 2007.

55 C. Subramanian, K.N. Stratford, T. P. Wilks and L. P. Ward, On the design of coating systems: Metallurgical and other considerations, Tribology International 41 (2008) 269–281.

56 Shunyan Tao, Zhijian Yin, Xiaming Zhou, Chuanxian Ding, Sliding wear characteristic of Al_{2O3} and Cr_{2O3} coatings against copper alloy under severe conditions, Tribology international 43 (2010), 69-75.

57 Anthony R. Vest, Solid state chemistry and its application, Wiley publication.

58 I.J Polmear, Light alloys-Metallurgy of the light metals, Edward Arnold, ISBN 0-340-49175-2.

59 Gwidon W. Stachowiak, Andrew W. Batchelor, Engineering Tribology, Butterworth Heinemann publications.

60 Piston ring Tribology by Peter Andersson, Jaana Tamminen & Carl-Erik Sandström.

61 Federal-Mogul Kolbenringe Kurbelgehäuse (piston rings / crankcases). Sonderdruck aus (reprinted from) ATZ/MTZ - Supplement Shell Lexicon Verbrennungsmotor. This edition: Burcheid, Germany, 1998, Federal-Mogul Powertrain Systems, 32 p.

62 Glaeser, W. A. Materials for tribology. Amsterdam, The Netherlands, 1992, Elsevier Science Publishers B.V., Tribology Series 20, 260 p. ISBN 0-444-88495-5.

63 www.federalmogul.com/kori**handbook**/en/section_41.htm

64 Bhusan and Gupta 1991

65 Mollenhauer, K. (Ed.). Handbuch Dieselmotoren (Diesel engines / in German). Berlin,Germany, 1997, Springer-Verlag, 1023 p. ISBN 3-540-62514-3.

66 Radil, K. The influence of honing on the wear of ceramic coated piston rings and cylinder liners. Lubrication Engineering, 57(2001)7, pp. 10–14.

67 Rastegar, F. and Richardson, D. E. Alternative to chrome: HVOF cermet coatings for high horse power diesel engines. Surface and Coatings Technology, 90(1997)1–2, pp. 156–163.

68 Broszeit, E., Friedrich, C. and Berg, G. Deposition, properties and applications of PVD CrxN coatings. Surface and Coatings Technology, 11(1999)5, pp. 9–16.

69 Zhuo, S., Peijun, Z., Leheng, Z., Xinfu, X., Aimin, H. and Wenquan, Z. Multi-layer compound coating on cast iron piston ring by multi-arc and magnetron sputtering ion compound plating technique. Surface and Coatings Technology, 131(2000)1–3, pp. 422–427.

70 Haselkorn, M. H. and Kelley, F. A. Development of wear resistant ceramic coatings for diesel engines, SAE Proceedings of the Annual Automotive Technology Development Contractors Co-ordination Meeting, 1992, pp. 417–424

71 Dufrane, K. F. Wear performance of ceramics in ring/cylinder applications. Journal ofthe American ceramic Society, 72(1989)4, pp. 691–695.

72 Kustas, F. M. and Buchholtz, B. W. Lubricious-surface-silicon-nitride rings for hightemperature tribological applications. Tribology transactions, 39(1996)1, pp. 43–50.

73 Federal-Mogul - Media - Press Release 8-aug-2011

74 New coating developments for high performance cutting tools,. Uhlmann, E. Wiemann, S. Yang,J. Krumeich,A. Layyous

75 Experimental study of wear interaction between piston ring and piston groove in a radial piston hydraulic motor (U.I. Sjodin, U.L.-O. Olofsson 2004)

76 Adhesion testing of thermally sprayed and laser deposited coatings (Anders Hjornhede, Anders Nylund .2004)

77 A rig test to measure friction and wear of heavy duty diesel engine piston rings and cylinder liners using realistic lubricants (John J. Truhan, Jun Qub, Peter J. Blau 2005)

78 Thermally sprayed titanium suboxide coatings for piston ring/cylinder liners under mixed lubrication and dry-running conditions (A. Skoppa, N. Kelling, M. Woydt, and L.-M. Berger 2007)

79 Frictional evaluation of thermally sprayed coatings applied on the cylinder liner of a heavy duty diesel engine: Pilot tribometer analysis and full scale engine test(S. Johansson, C. Frennfelt A. Killinger ,P.H. Nilsson, R. Ohlsson, B.G. Rosén 2010)

80 Wear measurement of the cylinder liner of a single cylinder diesel engine using a replication method (L.Gara ,Q.Zou, B.P. Sangeorzan,G.C. Barber, H.E. McCormick, M.H. Mekari 2010)

81 Frictional evaluation of thermally sprayed coatings applied on the cylinder liner of a heavy duty diesel engine: Pilot tribometer analysis and full scale engine test (S. Johansson, C. Frennfelt, A. Killinger, P.H. Nilsson, R. Ohlsson, B.G. Rosén. 2011)

82 Y. Xie, H.M. Hawthorne, Wear mechanism of plasma-sprayed alumina coating in sliding contacts with harder asperities, Wear 225–229 (1999) 90–103.

83 T. Kachele, Recent research results on predicting and preventing silt erosion, Proceedings of the First International Conference on Silting Problems in Hydropower Plants, October 1999, India, 1999

84 Y. Iwai a, T. Honda, H. Yamadaa, T. Matsubara, M. Larsson, S. Hogmarkd, Evaluation of wear resistance of thin hard coatings by a new solid particle impact test, Wear 251 (2001) 861–867

85 Yucong Wang, Simon, Tung, Scuffing and wear behavior of aluminum piston skirt coatings against aluminum cylinder bore, Wear 225–229 (1999) 1100–1108.

86 Rahul Premachandran Nair, Drew Griffin, Nicholas X. Randall, The use of the pin-on-disk Tribology test method to study three unique industrial applications, Wear 267 (2009) 823–827.

87 Garcia-Prieto, M.D. Faulkner, J.R. Alcock, The influence of specimen misalignment on wear in conforming pin on disk tests, Wear 257 (2004) 157–166.

88 Binshi Xua, Zixin Zhua, Shining Maa, and Wei Zhang, Weimin Liu, Sliding wear behavior of Fe–Al and Fe–Al/WC coatings prepared by high velocity arc spraying, Wear 257 (2004) 1089–1095.

89 Jeffree, C. E.; Read, Ambient- and Low-temperature scanning electron microscopy, Electron Microscopy of Plant Cells, London: Academic Press. pp. 313–413. ISBN 0123188806.

90 Karnovsky, A formaldehyde-glutaraldehyde fixative of high osmolality for use in electron microscopy, Journal of Cell Biology 27: 137A

91 Brauers, B. and Neuhäuser, H. J. K46 Nitrierschichten als Verschleißschutz für Kolbenringoberflächen - Werkstoffe, Erprobungsstand, Einsatzmöglichkeiten (K46 nitrided overlays as wear protection for piston

ring surfaces - materials, testing and applicability / in German). Burscheid, Germany, 1989, Goetze AG, Drucksache Nr. 893810 - 09/98. 18 p.

92 PVD Cr_xN coatings for tribological application on piston rings, Friedrich C.; Berg G.; Broszeit E.; Rick F.; Holland J., Surface and Coatings Technology, Volume 97, Number 1, December 1997 , pp. 661-668(8).

93 Federal-Mogul Kolbenringe Kurbelgehäuse (piston rings / crankcases). Sonderdruck aus (reprinted from) ATZ/MTZ - Supplement Shell Lexicon Verbrennungsmotor. This edition: Burcheid, Germany, 1998, Federal-Mogul Powertrain Systems, 32 p.

94 Coy, R. C. Practical applications of lubrication models in engines. Tribology International, 31(1998)10, pp. 563–571.

95 Sherrington, I. and Mercer, S. The use of topography-based parameters for the assessment and prediction of surface wear. Tribotest, 7(2000)1, pp. 3–11.

96 Gupta, P. On a multi-process wear model. Lubrication Engineering, 57(2001)4, pp. 19–24.

97 www.studyvilla.com/engines.aspx

98 Failure assessment of the hard chrome coated rotors in the down hole drilling motors. Khalil Ranjbar, Majid Sababi 2012, Engineering Failure Analysis 20 (2012) 147–155

99 Surface characterization of multiple coated H11 hot work tool steel by plasma nitriding and hard chromium electroplating processes. M.Soltanieh,H. ,AghajaniF.Mahboubi,Kh.A.Nekouee .2012, Vacuum, Volume 86, Issue 10, 27 April 2012, Pages 1470-1476

100 Effect of plasma spraying parameter on wear resistance of NiCrBSiCFe plasma coatings on austenitic stainless steel at elevated temperatures at various loads, Materials&Design, Volume36, April2012, Pages141-151, N.L. Parthasarathi, Muthukannan Duraiselvam, Utpal Borah

101 U. Helmersson, M. Lattemann, J. Bohlmak, A.P. Ehiasarian, J.T. Gudmundsson, Ionized Physical Vapor Deposition (IPVD): a review of technology and applications, Thin Solid Films, 513 (2006) 1.

102 J.S. Colligon, Energetic condensation: processes, properties and products, J. Vac. Sci. Technol. 13 (3) (1995) 1649.

103 D.M. Mattox, Film deposition using accelerated ions, Electrochem. Technol. 2 (1964) 295.

104 D.M. Mattox, Fundamentals of ion plating, J. Vac. Sci. Technol. 10 (1973) 47.

105 S. Aisenberg, R.W. Chabot, Physics of ion plating and ion beam deposition, J. Vac. Sci. Technol. 10 (1) (1973) 104.

106 S. Aisenberg, The role of ion-assisted deposition in the formation of diamond-like-carbon films, J. Vac. Sci. Technol. A8 (3) (1990) 2150.

107 C. Weissmantel, G. Reisse, H.J. Erler, F. Henny, K. Beuvilogue, U. Ebersbach, et al., Preparation of hard coatings by ion beam methods, Thin Solid Films, 63 (1979) 315.

108 D.M. Mattox, Surface effects in reactive ion plating, Appl. Surf. Sci. 48/49 (1991) 540.

109 K.S. Fancey, C.A. Porter, A.A. Matthews, The relative importance of bombardment energy and intensity in ion plating, J. Vac. Sci. Technol. A13 (2) (1995) 428.

110 Petrov, F. Adibi, J.E. Greene, W.D. Sproul, W.-D. Münz, Use of an externally applied axial magnetic field to control ion/neutral flux ratios incident at the substrate during magnetron sputter deposition, J. Vac. Sci. Technol. A10 (5) (1992) 3283.

111 T. Ohmi, T. Shibata, Advanced scientific semiconductor processing based on high-precision controlled low-energy ion bombardment, Thin Solid Films, 241 (1993) 159.

112 Bessaudou, J. Machet, C. Weissmantel, Transport of evaporated material through support gas in conjunction with ion plating: I, Thin Solid Films, 149 (1987) 225.